

THE EFFECT OF DIVE RECOVERY FLAPS
ON THE LIFT OF A TWO DIMENSIONAL SYMMETRICAL AIRFOIL
WITH CHANGES IN CHORDWISE LOCATION OF THE FLAPS

Thesis by

Lieutenant Commander Daniel K. Weitzenfeld, USN

Lieutenant Commander Robert J. Trauger, USN

and

Lieutenant Commander George R. Kronmiller, USN

In Partial Fulfillment of the Requirements
for the Degree of Aeronautical Engineer

California Institute of Technology
Pasadena, California

June, 1946

ACKNOWLEDGMENT

The authors are indebted to the staff of the Guggenheim Aeronautical Laboratory, California Institute of Technology.

In particular they wish to express their appreciation to Dr. Hans W. Liepmann and Mr. A. E. Puckett for their valuable help and criticism during the course of the investigation.

TABLE OF CONTENTS

<u>PART</u>		<u>PAGE NOS.</u>
I	Summary	
	Introduction	1
	Equipment	4
	Procedure	6
	Corrections and Precision	10
	Results and Discussion	18
	Conclusions	23
	Recommendations	24
	References	25
II	Figures	27

SYMBOLS

M	-	Free air Mach number
M'	-	Free stream Mach number
α_{th}	-	Angle of attack set by theodolite
α	-	Absolute angle of attack free air
C_l	-	Section lift coefficient
p	-	Static pressure at any wall orifice
p_o	-	Atmospheric pressure
Δ	-	Thickness coefficient
σ	-	Model size coefficient
q'	-	Free stream dynamic pressure
q	-	Free air dynamic pressure
$\frac{dc_l}{d\alpha}$	-	Lift curve slope per degree
C	-	Model chord in inches
h	-	Tunnel height in inches
l_1	-	Length from aero-center of model to rear orifice
l_2	-	Length from aero-center of model to front orifice
Γ	-	Circulation
$C_{l_{w.s.}}$	-	Section lift coefficient for lift measured in the working section
\bar{u}	-	free stream velocity feet per second
x,y	-	Coordinates of coordinate system
x_c	-	Percent chord
$\frac{dC_l}{dx_c}$	-	Rate of change of C_l along chord
C_p	-	Pressure coefficient

SUMMARY

It was desired in this investigation to determine the effect of the chordwise position of dive recovery flaps on the lift of a laminar flow, low drag, two-dimensional airfoil at high subsonic Mach numbers. Schlieren pictures were taken to relate the formation, extension and strength of shock waves to the measured lift. Tests were made on a four inch chord airfoil of section 65,1-012 at Mach numbers from .50 to .83, a Reynolds number of 1,600,000 at $M_0 = 0.7$, angles of attack from 1 to 3 degrees, and flap locations at 15%, 30%, and 45% chord; the flap is 10% of the chord.

The investigation was carried out by the authors at the Guggenheim Aeronautical Laboratory of the California Institute of Technology during the school year 1945-1946.

It was concluded that dive recovery flaps materially increase the lift of an airfoil, and there is an optimum flap location for maximum lift and one for maximum $\frac{dC_L}{d\alpha}$. Moreover, it was concluded that the formation and development of shock waves is directly related to the lift, but that the successive development of the shock wave pattern as a function of Mach number is independent of angle of attack or flap location; the Mach number for initial shock formation varies. Finally, in this tunnel where the thickness of the boundary layer is a large percent of the tunnel width the correction for non-uniform spanwise lift distribution must be investigated more carefully before absolute lift values can be computed.

INTRODUCTION

The problem of shock waves occurring on the wing of a plane at speeds less than that of sound, and subsequent large diving moment forces caused by these shock waves led to the use of dive recovery flaps. These flaps on full-size airplanes, when actuated by the pilot in a dive, or in pulling out of a dive allow the pilot at least enough control to overcome the large diving moment caused by the shock waves. These phenomena are related not just to the wing, but to the interrelation between the wing and the tail; recovery of the use of the tail as a control surface operated within the muscular strength of the pilot is inherent in the use of dive recovery flaps.

The first solution to this problem was made by trial and error. Large sized airplane models were fitted with dive recovery flaps as in reference 1 and tests made in wind tunnel. Tests were also made on actual airplanes under actual flight conditions. The position chordwise or spanwise, size, and angle of deflection were all parameters of these investigations. In reference 1 the flaps were placed at 33% of the wing chord for structural reasons which could necessarily be another consideration.

Due to the exigencies of the situation final results were desired, and no theory or empirical data were derived. The theory of the effect of increasing Mach number on the lift, drag, and moment of an airfoil without flaps is fairly well defined by references 2, 3, 4, 5, 6, 7, and others. A large amount of empirical data has been obtained to substantiate these theories. Moreover, some relations of the formation and type of shock waves to the pressure distribution have been established in reference 3.

In general, the experimental data is affected by errors due to wind tunnel wall interference. Allen and Vincenti in reference 8 have obtained theoretical corrections for wind tunnel parameters which agree fairly well with empirical data up to wind tunnel choking. However, these corrections apply to fairly large wind tunnels and to force measurements or chordwise pressure measurements on the body itself. The correction to the lift for the length of the working section has been satisfactorily worked out. There is no satisfactory theory to correct for the non-uniform spanwise distribution. J. A. Preston (reference 9) made an investigation of the effect of the boundary layer on the lift distribution, but his work is not completely applicable to the tunnel in which the subject experiment was conducted. During the course of the investigation it was discovered that a more accurate investigation of this effect should be made.

In this investigation it was desired to determine the effect of dive recovery flaps on the lift of two-dimensional laminar flow airfoil at low angles of attack and various Mach numbers for three chord positions: 15%, 30% and 45% of chord. These positions are considered to cover the region in which actual dive recovery flaps are used on airplanes. It was also desired to show the effect of the flap on the formation of shock waves by the use of schlieren photographs, and then correlate the actual data to the pictures.

Lift measurements were made by integrating the pressures over the top and bottom of the tunnel. This method has some advantages for small models in that it does away with balance strut and clearance

problems. However, the measurement itself was inaccurate because it does not measure all the lift lengthwise in the tunnel, and it does measure the decrement of lift due to the comparatively large boundary layers on the sides of the tunnel and their effect on the spanwise lift distribution of the airfoil. A correction was made for the fraction of the lift not measured on the top and bottom walls, but no correction was made for the non-uniform spanwise lift distribution. Therefore, the lift coefficients reported are essentially spanwise averages, and are lower than the true section lift coefficient on the tunnel C.L. It was desired to reduce the data primarily to show the increment of lift due to the flaps and the rate of change of this increment along the chord. However, it was also desired to compare the data and schlieren pictures to miscellaneous investigations such as included in references 11, 3, 5, and 6.

The tests were conducted in a two-dimensional, open return, induction type wind tunnel having a test section of one by ten inches cross-section by twenty inches long. It is capable of giving a Mach number of 0.87 with no model installed.

The tests were made at the Guggenheim Aeronautical Laboratory of the California Institute of Technology in March, April, and May of 1946. The tests were made in collaboration with the tests made for the investigation of reference 12.

EQUIPMENT

The wind tunnel in which this investigation was carried out is of the two-dimensional, free air entrance, open return, induction type. The details of its construction are described in references 13 and 14. A picture of the tunnel is shown in Fig. 1. The working section is 20" long with a cross section tapering from .9" x 10" at the entrance to 1.0" x 10" at the beginning of the diffuser section. The taper is to allow for the growth of boundary layer along the walls. In this investigation it was necessary to replace the tapered floor and roof blocks of the working section of the tunnel. These blocks contained the drilled holes into which were inserted the pressure tubes. The blocks have been made of a laminated plastic, but had become so warped by dimensional instability that the glass side walls no longer fitted snugly. In addition, the warping caused a misfit of the bell-mouth on the tunnel entrance which gave rise to considerable turbulence. For these reasons the plastic blocks were replaced by machined brass blocks.

Previous surveys of velocity had been made in the working section and it had been determined that the flow was satisfactorily uniform vertically in the working region. The maximum Mach number attainable with no model in the tunnel was about .87 and with a model in the tunnel this value was reduced to about .82.

The three models used in this investigation were constructed of machined brass. All had an NACA 65₁ - 012 section, with 4" chord and each contained a flap of 10% chord length located respectively at 15%,

30%, and 45% of the chord from the leading edge. The flaps were so constructed as to recess flush with the lower surface when retracted, and to extend at an angle of 45° to the chord line when actuated by a tug on a small wire leading from a lug on the side of flap, downstream against the glass side wall (in the boundary layer). The wire was led out of the tunnel in the diffuser section through a small hole drilled in the side wall.

An ordinary theodolite was used in conjunction with a small surface reflecting mirror attached to an extension shaft on the airfoil support trunnions to determine angle of attack. A schematic diagram of the angle of attack measuring device is shown in Fig. 3.

The schlieren equipment contained two alternate sources of light, one an ordinary bulb, and the other a spark with a 10^{-4} second exposure. The spark source was used to take all pictures. A schematic diagram of the schlieren equipment is shown in Fig. 4.

Additional details of the model construction, the schlieren equipment, and the angle of attack mechanism may be found in reference 12.

PROCEDURE

It was desired to obtain data in two categories; the flap retracted condition and the flap set condition. The term flap set is to be construed as meaning that the flap was locked in the down position at the beginning of the run, ($M = 0$), and then the air speed was increased to the desired Mach number. Considerations of the details of operation such as cleaning the glass sidewalls of the tunnel and retracting the flap led to the adoption of the sequence of operations hereinafter described.

The designated model, properly gasketed, was attached to the control wire by which the flap was actuated. The model trunnions were then inserted into the bearings provided and the bearings themselves inserted into the drilled fitted holes in the glass side walls. The side walls were then pressed in against the model by tightening the screws provided for that purpose until the model was lightly held by friction alone. Then the model was tapped lightly until it was approximately at an angle of attack of 0° as determined by measurements made with a steel rule. Next a considerable pressure was set up on the side walls to keep the airfoil from slipping.

With the airfoil now set and the theodolite in position and leveled, the mirror was slipped onto the integral shaft protruding from the airfoil through the trunnion and the mirror was rotated by hand until it could be lined up at approximately zero on the angle of attack scale. The mirror was then fixed in this position relative to the airfoil by a set screw. The reading taken through the theodolite then was recorded as the reference reading.

The bellmouth was then installed and the tunnel started. When the desired Mach number had been obtained by manipulation of the compressor by-pass valve, a prearranged signal was given to the various stations and the operations of taking the schlieren photos, and recording the manometer liquid heights by colored pencil on a graph paper backing were concluded as expeditiously as possible.

If the flaps had been down on a previous run and it was desired to obtain a flap retracted run it was necessary to shut the tunnel down, slack off on the control wire and press the flap back into its recessed position by means of a thin tool inserted through the bellmouth for this purpose. The inefficiency of this procedure was offset by the fact that it was necessary to stop the tunnel at frequent intervals anyway to permit the compressors to cool; the runs were so arranged as to coincide with these intervals insofar as was possible.

With the runs completed at one angle of attack, the bellmouth was removed, the side wall clamps loosened to permit forced movement of the airfoil, and the airfoil then gently tapped with a wooden stick until it had shifted to the next desired angle as determined by the theodolite.

Then the walls were again clamped, the bellmouth reinstalled and another series of runs were executed at this new angle.

When runs at all desired angles had been obtained by these methods, the tunnel was disassembled sufficiently to remove the old model and replace it with the new model. Flap up runs were interspersed with the flap set runs to permit correlation of the reference angles to

the absolute angle by considerations of the fact that a plot of C_e vs. α for a symmetrical airfoil must pass through 0,0.

A brief discussion of operating difficulties in the tunnel may be of interest to indicate the nature of some of the problems encountered. The most serious problem from a standpoint of time and expense was the breakage of the glass side walls. Four sides were broken during the experiment. Since none of the sides were broken during the actual operation of clamping up the sides of the tunnel against the airfoil, but instead occurred during, or after the runs had been completed, it was felt that the breakage could not be regarded as resulting from rough handling. All failures were starting at the ends of the elliptical slot and radiating outward as was to be expected. An elementary analysis indicated the stress to be excessive in that region. For this reason the side walls were redesigned to contain a circular hole, thus reducing the stress concentration by about one-half, and the airfoil models were machined down to allow the use of a thin rubber gasket on each side to distribute the load more evenly. The problem yielded to this treatment.

Another problem was that of the manometer liquid. Alcohol was used for the first few runs, which were all either with no flaps or with flaps at very low angles of attack. Lead perchlorate was then used and it, too, was found to be too light to keep the pressure differences within the 40" limit of the manometer board at the highest angles of attack desirable. Other liquids investigated had an adverse effect on the properties of rubber, or steel or both, so that mercury was used in all the runs at 30% chord, 45% chord and at 2 and 3 degrees for 15% chord. Had time permitted, the construction

of an all glass manometer would have been desirable in order to use tetraethyl bromide. However, this would also have meant that the manometer board would have had to be redesigned and made much larger, or mercury would have had to have been used anyway.

Because the schlieren pictures were taken with a spark source it was necessary to darken the room to take pictures and to change photographic plates. This procedure obviously hampered operations.

From the readings recorded on the graph paper behind the manometer tubes, pressure differences between matching pairs of orifices, top and bottom, were measured. These differences Δp , were then plotted on a graph vs. distance along tunnel axis, and the area under the curve was integrated by a planimeter to determine lift. The dynamic pressure, q , was determined by means of a measurement of the stagnation pressure, p_0 , which in this case was atmospheric, with the aid of the relation

$$q/p_0 = \frac{\gamma}{2} \frac{p}{p_0} M^2$$

With q and L thus determined and p_0 determined from the barometer, C_L was evaluated. Additional curves were then cross plotted as indicated under Results.

CORRECTIONS AND PRECISION

Measurement of the free stream Mach number directly was impossible due to the size of the wind tunnel. With no model in the tunnel a lengthwise pressure calibration showed that a measurement at one of the middle orifices would give the true free stream Mach number. However, insertion of the model influenced all orifices after the second orifice.

Measurement of the Mach number was made at the second orifice by measuring $p - p_0$ on a manometer board using a scale to read directly in Mach number by use of the following equation:

$$(p - p_0) = p_0 \left(1 + \frac{\gamma - 1}{2} M^2 \right)^{\frac{\gamma}{\gamma - 1}} - 1 .$$

This Mach number was corrected to the free stream Mach number by plotting a curve of ΔM versus uncorrected M ; this correction was additive in all cases. This curve was obtained from calibration runs made with no model in the tunnel. The Mach number at the second orifice was computed from the p/p_0 relationship:

$$p/p_0 = \left(1 + \frac{\gamma - 1}{2} M^2 \right)^{\frac{\gamma}{\gamma - 1}}$$

Solving for M for air:

$$M = \sqrt{5 \left[\left(\frac{p_0}{p} \right)^{.286} - 1 \right]}$$

The true free stream Mach number was also computed by the same relationship from the p/p_0 near the middle orifices and the difference plotted.

For a p/p_0 of 0.722 at the second orifice a p/p_0 of 0.715 was obtained in the free stream. This gave an uncorrected Mach number of

0.698 and a corrected one of 0.709, a difference of plus 0.011.

It was found that at any Mach number below 0.52 no correction was necessary.

As the direct reading uncorrected Mach scale was based on a standard p_0 (745 mm Hg.) an investigation of the effect of the change of p_0 was carried out. This curve was plotted, but over the period of the tests the correction to Mach number was never more than $\pm .001$ so that this correction was neglected.

An investigation of the effect of the height of the mercury in the Mach meter was also made. However, at the highest Mach numbers this effect was only to change the zero reading of the Mach number $-.002$ so that this also was neglected.

A correction for wind tunnel wall interference was made to the free stream Mach number, using the method of formula 33, page 72, in reference 8 using a σ of .033, a μ of .221 without flaps, and a μ of .348 with flaps extended. The Mach number as read should be accurate to ± 0.002 . Any additional error due to the corrections should not be more than $\pm .003$ so that the Mach number is correct to $\pm .005$.

On obtaining values of C_L with no flaps quite a substantial difference in the values and the slope of the lift curve from those in reference 15 was obtained. Application of wind tunnel wall corrections using the first three terms in formula 62, page 62 of reference 8 increased this difference. In previous work in this tunnel it had been assumed this was due to improper measurement of the angle of attack. Reference 12 showed that this was not so, but

that part of the difference was due to the fact that all the lift of model was not being measured, and part to the non-uniform spanwise lift distribution.

The reason for this was due to two things; the method of measurement of the lift, and the effect of the tunnel side wall boundary layers on the velocity and pressure distribution over the whole width of the model. R. W. Bell, in reference 10 showed that in incompressible flow for a lifting line vortex:

$$\frac{L_{w.s.}}{L} = \frac{2}{\pi} \left[\tan^{-1} e^{\frac{\pi l_1}{h}} - \tan^{-1} e^{-\frac{\pi l_2}{h}} \right]$$

See Fig. 5a

and for a vortex sheet:

$$\frac{C_{l_{w.s.}}}{C_l} = \frac{\sum_{\text{chord}} A(x) \frac{\Delta p(x)}{\rho}}{\sum_{\text{chord}} \frac{\Delta p(x)}{\rho}}$$

where L_{ws} is the lift measured in the working section, L is the total lift, $\Delta p(x) = p_l - p_u$

and p_l = pressure on wind lower surface at position (x) along chord

p_u = pressure on wing upper surface at position (x) along chord.

and

$$A(x) = \frac{2}{\pi} \left[\tan^{-1} e^{\frac{\pi(l_1-x)}{h}} - \tan^{-1} e^{-\frac{\pi(l_2+x)}{h}} \right]$$

See Fig. 5b

Calculation of the percentage of lift measured in the wind tunnel in use by the first method gave a percentage of lift measured 91.0% and by the second method of 90.0%.

The method was corrected for compressibility by using the Prandtl-Glauert approximation. Application of this approximation to a wind tunnel consists of substituting:

$$X \text{ comp.} = X \text{ in comp.}$$

and
$$Y \text{ comp.} = \frac{Y \text{ incomp.}}{(1 - M^2)^{1/2}}$$

The equation then became

$$\frac{L \text{ w.s.}}{L} = \frac{2}{\pi} \left[\tan^{-1} e^{\frac{\pi l_1}{h\sqrt{1-M^2}}} - \tan^{-1} e^{\frac{-\pi l_2}{h\sqrt{1-M^2}}} \right]$$

as
$$h \text{ incomp.} = h \text{ comp. (the actual } h) \times \sqrt{1 - M^2}$$

Solution of this equation showed that for increasing Mach number a greater percentage of lift was measured. This percentage went from 91% at $M = 0$ to 97% at $M = 0.70$.

Plotting of the $\frac{dC_e}{d\alpha}$ vs. M curve (Fig. 9) showed that for this model only 67% of the lift at $M = .2$ was being measured and 78.6% at $M = .5$. At $M = .2$ then, 23.0% of lift and at $M = .5$, 16.4% of the lift was still unaccounted for.

In reference 9, J. A. Preston showed that

$$\frac{\Delta \alpha}{\alpha} = \frac{\Delta C_e}{C_e} = \frac{4 C \delta^*}{l^2} \times 100 \%$$

where C is the chord length of the model,

l is the width of the tunnel,

δ^* is the displacement thickness.

$$\delta^* = \delta \int_0^1 \left(1 - \frac{u}{\bar{u}}\right) d\left(\frac{y}{\delta}\right)$$

$\Delta \alpha$ is the angle of attack induced by the vortex.

Using the logarithmic velocity profile of reference 16, page 15,
formula 44:

$$\begin{aligned}\frac{u}{u} &= \left[1 - 4.15 (C_f)^{\frac{1}{2}} \log_{10} \left(\frac{\delta}{y} \right) \right] \\ &= \left[1 + 4.15 (C_f)^{\frac{1}{2}} \log_{10} \left(\frac{y}{\delta} \right) \right]\end{aligned}$$

substituting

$$\begin{aligned}\delta^* &= \delta \int_0^1 \left[1 - 1 - 4.15 (C_f)^{\frac{1}{2}} \log_{10} \left(\frac{y}{\delta} \right) \right] d \left(\frac{y}{\delta} \right) \\ &= \delta \int_0^1 - \frac{4.15}{4.6052} (C_f)^{\frac{1}{2}} \ln e \left(\frac{y}{\delta} \right) d \left(\frac{y}{\delta} \right) \\ &= \delta \left(-\frac{4.15}{4.6052} [C_f]^{\frac{1}{2}} \right) (\ln e 1 - 1) \\ &= .9 \delta (C_f)^{\frac{1}{2}}\end{aligned}$$

For a Mach number of 0.2 the Reynolds number is 460,000, which
from reference 16 gives a C_f of 0.00513.

Then $\delta^* = .0645 \delta$

The boundary layer was computed from $\delta = 0.377 \left(\frac{v}{u x} \right)^{\frac{1}{2}} x$

where X was the distance from the front end of the working section.

For this wind tunnel $\delta = .38 \left(\frac{1}{u} \right)^{\frac{1}{2}}$ at the quarter chord
position of the model.

For a Mach number of 0.2, $\delta = 0.130$ inches. The boundary
layer actually determined in the tunnel with no model and at a Mach
number of 0.2 was 0.15 inches; the discrepancy was probably due to
the entrance conditions. It was assumed for the computation that the
boundary layer started at the entrance of the working section where
actually it started on the bellmouth, thus increasing the width

thickness of the boundary layer at the point in question.

Using 0.15 as the boundary layer thickness at $M = 0.2$

$$\delta^* = .0097$$

and $\frac{\Delta C_e}{C_e} = 16\%$;

at $M = .5$, $\delta \approx .11$ by the equation above: Allowing for the entrance conditions $\delta = .12$.

For $M = 0.5$, $R_N = 1,150,000$

and $(C_f) = .0043$

then $\delta^* = .0079$

This gives $\frac{\Delta C_e}{C_e} = 12.7\%$.

If the Prandtl-Glauert correction is applied to Preston's formula,

$$C_{incom} = C_{comp}$$

$$l_{incom} = l_{comp}, \text{ (the true } l \text{) } \times \sqrt{1 - M^2}$$

and $\frac{\Delta C_e}{C_e} = \frac{4c\delta^*}{l^2(1-M^2)}$

A summary of the lift measurement is as follows:

Mach No.	% Lift Measured	Correction for Length of Working Section	Correction for Boundary Layer	Comp. Correction for Boundary Layer	Unaccounted for
.2	67	9.5	16	{ 16.7 17.0 }	7.5
.5	78.6	7.0	12.7		1.7
.7	82.4	4.0	11.2		2.4

The correction for the length of the working section was assumed to be accurate. Lift coefficients were corrected for the wind tunnel walls and for this working section correction. The correction as determined by Preston is evidently of the right order. However, his initial assumption of a pair of vortices, one at a distance δ^* from

the wall, the other the image in the wall, is evidently very good for a fairly large tunnel but has its limitations when the tunnel size is reduced. The value of the computed $\frac{\Delta \alpha}{\alpha}$ applies only at the center of the tunnel. In a small tunnel the increase of $\frac{\Delta \alpha}{\alpha}$ going spanwise from the center to the displacement thickness would materially affect the decrement of lift. This consideration would give an additional correction, and it would be in the right direction. Moreover, no effect of compressibility is taken into consideration in Preston's original assumption. If the Prandtl-Glauert correction is applied the correction becomes too large at higher Mach numbers.

Consequently, it is evident that a boundary layer correction should be made, but that more investigation is necessary. As the subject of this paper is concerned more with comparative than with absolute values, and because of the questionable accuracy, this correction was not made.

No comparison in precision can be made as regards to absolute values. Each wall pressure measurement should be accurate within 0.5% q . Pressure differences with no model in were never more than one millimeter of mercury; no corrections to the wall pressures were made as this difference is included in the estimate above. Integration of these pressures by planimeter should also be accurate to 0.5% q so that C_p should be accurate within 1.0%.

The angle of attack measurements by the theodolite are within $\pm .03^\circ$, which takes into account the slippage of the model due to aerodynamic forces and the method of holding the flaps down. Consequently, the precision of relative angles is within this same error.

The theodolite angle of attack was corrected to absolute angle by making runs with flaps up at a certain Mach number, entering the C_p vs. α curves of reference 12, and getting an absolute angle of attack. These angles were corrected to free air angles by formula 64b, page 62, reference 8 using only the first two terms. The absolute angle of attack is correct within 0.1° .

The sensitivity of the schlieren equipment used is very hard to define accurately. Possibly by looking at the boundary layer in the pictures and by a comparison to the pictures obtained in reference 3 it can be seen that this equipment is only moderately sensitive. As the sensitivity was enough to show the heated air rising from one's hand, the difficulty may be in the method of taking the pictures.

The relative humidity throughout the investigation was approximately 50%. No definite condensation shocks were noticed in the schlieren screen. No effort was made to evaluate the effect of water vapor and dust in the air on the formation of the shock waves.

RESULTS AND DISCUSSION

The lift coefficients derived by the method outlined in PROCEDURE were plotted on Fig. 6 and curves drawn. Curves approximating the Prandtl-Glauert correction and the Karman-Tsien correction were drawn from the same point on two of these curves for comparison. The discrepancy is probably due to the decrement of measured lift which would be less at high Mach numbers. This then would indicate that the shape of these curves, if corrected properly, would approach the Karman-Tsien or Prandtl-Glauert approximations. Moreover, the Karman-Tsien and the Prandtl-Glauert approximations are not valid after the flow is locally supersonic, which would account for some of the difference.

The $C_{l\max}$ of the lower curves on Fig. 6 agree very closely with the curve of $C_{l\max}$ vs. Mach number in reference 13.

The highest Mach number points are the limiting values for this tunnel. At this point choking occurred and no higher Mach numbers were obtained. These choking points agree very well with the curve in Fig. 5, reference 11.

Figure 7a is a faired curve plot of C_l vs. α from the curves in Fig. 6. The C_l vs. α curves for this airfoil without flaps from reference 12 are also plotted. In fairing the curves, an attempt was made to have all curves for any one flap location intersect on the C_l equal zero line.

The curves in most cases are straight lines below the stalled position. At these relatively high angles of attack, the stall at the higher Mach numbers is gradual. Two exceptions to the straight line curves are the curves with the flap at 30% chord at Mach number of .55 and .60.

Fig. 7b shows a plot of the slopes of the curves in Fig. 7a for two Mach numbers vs. the flap location. This shows that there is a maximum slope to the lift curve somewhere just aft of the 30% chord position. This position of maximum slope is only slightly affected by Mach number below the stall.

Figs. 8a, 8b, 8c, 8d, 8e are plots of the original data points on a C_l vs. flap location graph, at various angles of attack and various Mach numbers. Curves were faired in between the points. In fairing this curve it would have been possible to fair in a maximum somewhere between 30% chord and 45% chord, but a study of the schlieren pictures indicates the maximum condition is slightly beyond the 45% chord position. The curves in general fall in the same pattern below the stall. After the stall has been reached, i.e., at the higher Mach numbers, the curves cross those of lower Mach numbers.

Fig. 9 is a plot of $\frac{dC_l}{d\alpha}$ vs. Mach number and includes the theoretical Prandtl-Glauert curve, and the curve for no flaps from reference 12. The curve for some optimum location of the flap, again somewhere aft of 30% chord, is materially larger than the curve for the no flap position.

The difference between the no flap curve and the theoretical curve has already been discussed in CORRECTIONS. Because of this difference, all curves would be moved upward to give absolute values, but the relative differences would remain approximately the same.

Fig. 10 is a plot of the change of C_l from the model with no flaps for the three flap locations at various Mach numbers vs. angle of attack.

For corresponding Mach numbers the increment of lift increases quite rapidly when moving the flap from 15% chord to 30% chord, and is still increasing slightly as the flap is moved aft to 45% chord. This is another indication that the maximum lift position for the flap is slightly aft of the 45% chord location.

Fig. 11 is a plot of the change of C_L from the model with no flaps at various angles and Mach numbers vs. the flap location. This plot shows that the maximum lift increment in all cases has yet to be reached. It also shows that at a constant Mach number increasing the angle of attack decreases the increment of lift obtained. This indicates that the increment of lift obtained in increasing the angle of attack with the flaps extended is less than the increment obtained when the angle of attack is increased using no flaps.

The slopes of these curves at each flap location are practically the same. A plot of the slopes vs. the flap location in Fig. 12 shows that the rate of change of slope decreases very rapidly as the 45% chord position is approached. Fig. 12 shows again that the maximum increment of lift would occur slightly aft of the 45% chord position.

Fig. 13 is a survey of the formation of shock waves on the model with the flap at 15% chord, 30% chord, and 45% chord at an angle of attack of three degrees and from just after the shock wave starts up to wind tunnel choking. This is a representative set of pictures as the shock waves form in the same manner for all angles of attack. The sequence of formation and movement of the shock waves is as follows: A small laminar shock first appears just aft of the nose. This forma-

tion is similar to that reported in reference 13 for high angles of attack. This agrees with reference 13 as these angles, although small in reference to the geometric angle, are relatively large in reference to the angle of zero lift.

The second shock occurs at about 30% chord at a Mach number of about .05 to .07 higher. At first this also is a laminar shock. In some cases the formation of this second shock is preceded by the formation of many small shocks just ahead of it. This phenomenon may have caused the irregularities in the two lift curves in Fig. 7a. As the Mach number increases both shocks move aft on the surface. The first shock wave tends to move away from the surface an appreciable distance while the second shock is still laminar. This phenomenon can be seen at 30% chord, $M = .648$. In some cases the second shock wave becomes a forked shock wave, as shown in this same picture and in the upper right hand picture of Fig. 13.

As the Mach number is increased the second shock moves aft and goes from a laminar type shock wave to a turbulent type shock wave. This type of wave is recognized by the triangular base and the inclination downstream (See reference 3). The last pictures show the shock extending to the tunnel wall, thus indicating choking of the wind tunnel.

Reference 3 notes that movement aft and consequent strengthening of the shock wave causes the peak negative pressure to move aft on the airfoil. This increases the area of the C_p vs. X_c curve. This in effect increases the lift coefficient of the airfoil.

Moving the flap chord position aft hastens the formation of the shock as is seen in the left hand pictures in Fig. 13. At constant Mach number the strength of the shock wave increases as the flap location is moved aft. However, it is evident that the change of strength is more pronounced in going from 15% chord to 30% chord than from 30% chord to 45% chord. This conclusion agrees with the data presented in Fig. 8.

Fig. 14 is a survey of the formation of shock waves on the model with the flap position at 45% chord in increasing the angle of attack from 1° to 3° . The formation of the shock waves at a constant angle of attack when the Mach number is increased is similar to the previous discussion. Increasing the angle of attack at a constant Mach number hastens the formation of the waves, which in effect increases the lift.

Fig. 15 shows some schlieren pictures of the model with no flaps. Again the formation of the shock waves is similar. Comparison between Fig. 15 and Fig. 13 shows that the formation of the shock waves occurs at a much lower Mach number when flaps are used due to the effective camber caused by the flaps and the higher induced velocities on the upper surface of the airfoil.

CONCLUSIONS

Dive recovery flaps materially increase the lift of an airfoil at high Mach numbers and low angles of attack. The maximum lift is obtained slightly aft of the 45% chord location; the maximum $\frac{dC_l}{d\alpha}$ is obtained slightly aft of the 30% chord location. The rate of change of C_l as the flap is moved along the chord is not materially affected by changes in angle of attack or Mach number. The flaps and movement of the flap location aft hasten the formation of shock waves, but the development of the shock pattern and movement of these shock waves are not affected by change in flap location or change in angle of attack, although they are affected by Mach number. The shock wave configuration is directly related to the lift; predictions of change in lift can be made by a study of schlieren photographs of the shock waves.

Measurement of the lift by integrating the pressures over the top and bottom of the tunnel for this type tunnel is not adequate to give absolute values of lift without further investigation.

RECOMMENDATIONS

1. The accuracy of the results may be increased by redesigning the manometer board to allow the use of alcohol or lead perchlorate as the fluid for high lift coefficients.
2. The schlieren photographs may be bettered by changing the method of taking photographs. A closed camera with a shutter so that data recording may be done with the lights on, and no extraneous light can get on the film is required.
3. The wind tunnel working section should be redesigned to permit cleaning the glass without removing the model. Substitution of a steel plate with a mirror finish on one side for one of the glass sides should be considered. This would result in the complete redesign of the Schlieren equipment, but would have many advantages; the main one is that it could be used for a working side.
4. It is feasible that a balance system and a simpler, more accessible angle of attack mechanism could be designed for the wind tunnel.
5. An investigation of the boundary layer effect on the pressure coefficient should be made with models of various lengths.
6. An extension of these results should be made, varying the length of the flap and varying the deflection angle.
7. Some investigation should be made of the effect of water vapor and/or dust particles on the formation and development of shock waves.

REFERENCES AND BIBLIOGRAPHY

1. Hamilton, W. T., and Brody, L. E.; "High Speed Wind Tunnel Tests of Dive Recovery Flaps on a 0.3 Scale Model of the P-47-D Airplane" NACA ACR # 5D19, May 1945.
2. Stack, John, Lindsey, W. F., Littell, R. E.; "The Compressibility Burble and the Effect of Compressibility on Pressures and Forces Acting on an Airfoil" NACA TR # 646.
3. Liepmann, H. W.; "Investigations of the Interaction of Boundary Layer and Shock Waves in Transonic Flow" GALCIT Report May 1946.
4. Liepmann, H. W., and Puckett, A. E.; "Introduction to Aerodynamics of a Compressible Fluid" GALCIT Course 1946.
5. von Karman, Th; "Compressibility Effects in Aerodynamics" Jour. Inst. Aer. Sc. July 1941.
6. Tsien, Hsue-shen, and Lees, Lester; "The Glauert-Prandtl Approximation for Subsonic Flows of a Compressible Fluid" Jour. Aer. Sc. April 1945.
7. Taylor, G. I., and Maccoll, J. W.; "The Mechanics of Compressible Fluids" Vol. III Aerodynamic Theory, W. F. Durand, Durand Re-printing Committee, GALCIT.
8. Allen, H. Julian, and Vincenti, Walter G.; "Wall Interference in a Two-Dimensional Flow Wind Tunnel With Consideration of the Effect of Compressibility" NACA ARR # 4K03 December 1944.
9. Preston, J. A.; "The Interference on a Wing Spanning a Closed Tunnel, Arising from the Boundary Layers on the Side Walls, With Special Reference to the Design of Two-Dimensional Tunnels" R. & M. 1924.
10. Bell, R. W.; "Lift Measured from Floor and Ceiling of Two-Dimensional Tunnel" GALCIT PAPER 1945.
11. Byrne, Robert W; "Experimental Constriction Effects in High Speed Wind Tunnels" NACA ACR # L4L07a, December 1944.
12. Parker, J. F., Anderson, J. B., Tunnell, R. W., and Vincent, H.; "The Effect of Sudden Extension of a Dive Recovery Flap on the Aerodynamic Characteristics of a Symmetrical Airfoil in Two-Dimensional Flow" Thesis, GALCIT June, 1946.
13. Chambers, L. S., Doll, R. E., Harrell, D. A.; "An Investigation of the Effects of Angle of Attack and Airfoil Model Size in the Occurrence of Shock Waves in a Two-Dimensional Tunnel" Thesis, GALCIT June, 1944.

14. Leydon, J. K., Miller, W. B.; "An Investigation of Wind Tunnel Wall Effects at High Mach Numbers" Thesis GALCIT June 1945.
15. Jacobs, Eastman N.; "Measured Velocity Distributions and Lift Curves For Various Airfoil Sections" NACA Conf. Report in loose-leaf form.
16. Karman, Th. v.; "Turbulence and Skin Friction" Jour. Aer. Sc. January 1934.
17. Heaslet, Max A.; "Critical Mach Numbers of Various Airfoil Sections" NACA ACR # 4G18 July 1944.
18. Army Air Forces TR # 4524 Revision 1, "Compressibility Phenomena as Related to Airplane Structural Design" July 7, 1942.

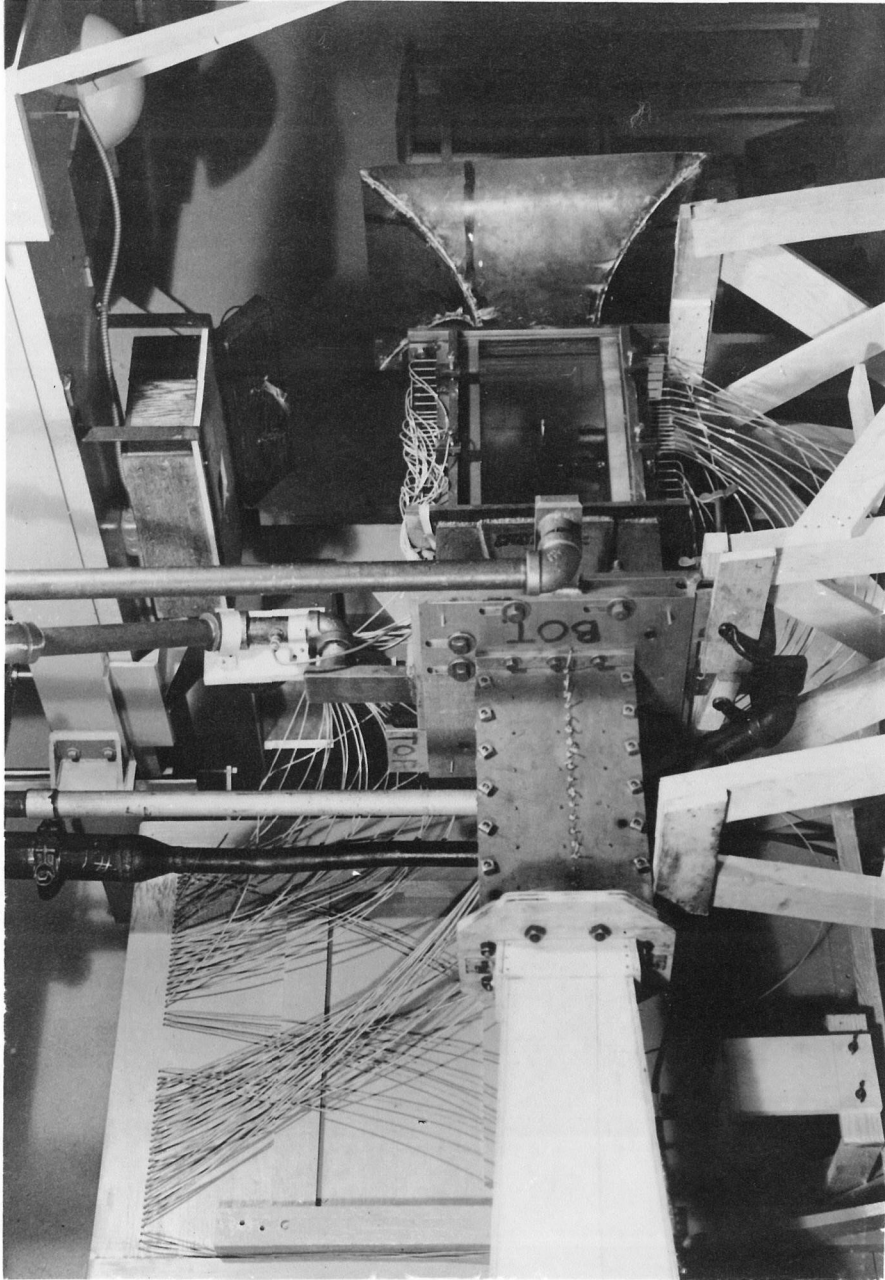
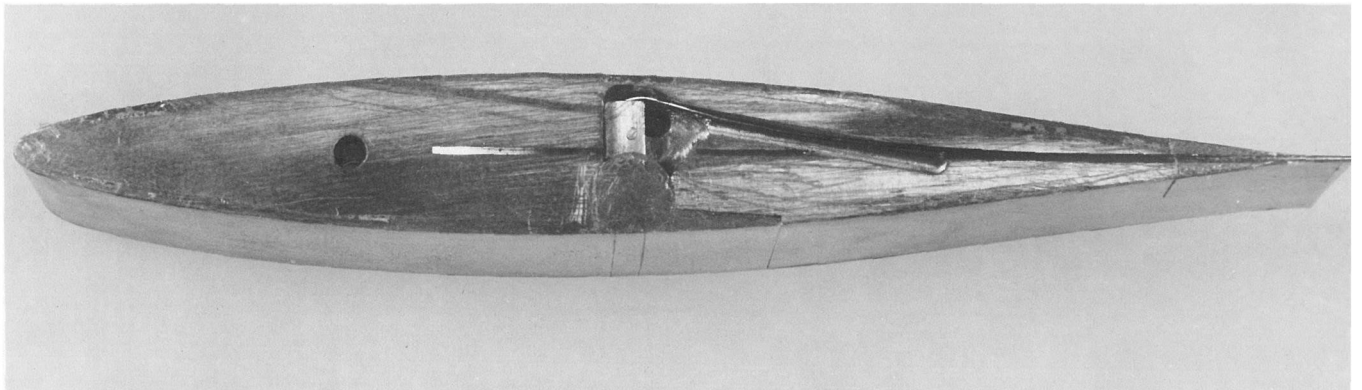
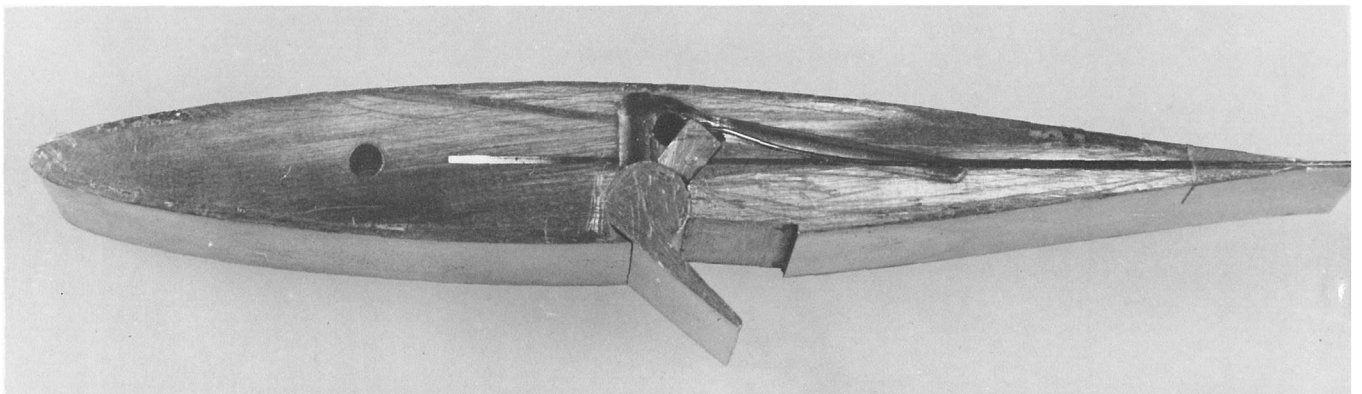


Fig. 1
Wind Tunnel



Flap retracted



Flap extended

Fig. 2

Model of NACA Airfoil 65, 1-012
Equipped with Dive Recovery Flap

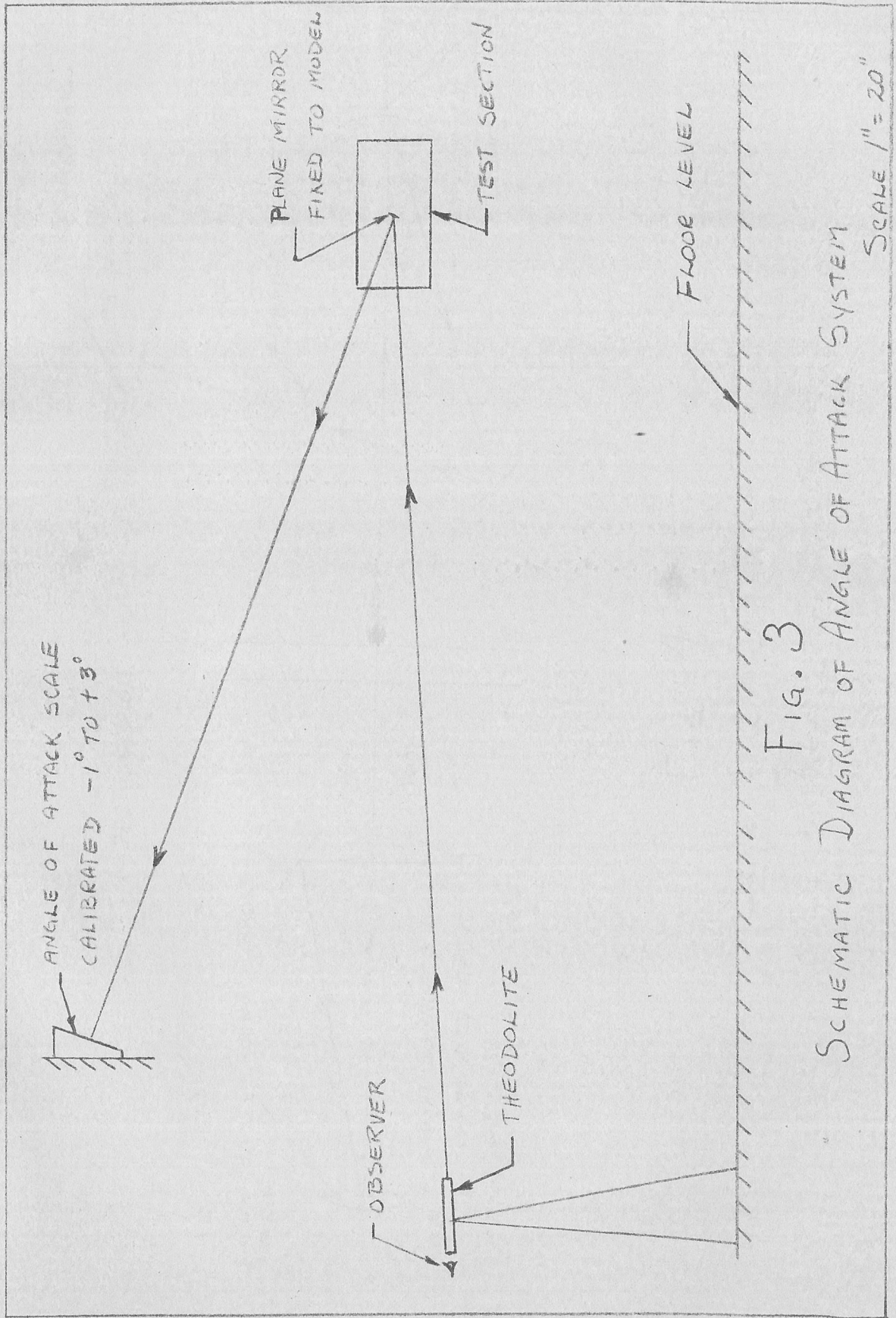


FIG. 3

SCHEMATIC DIAGRAM OF ANGLE OF ATTACK SYSTEM

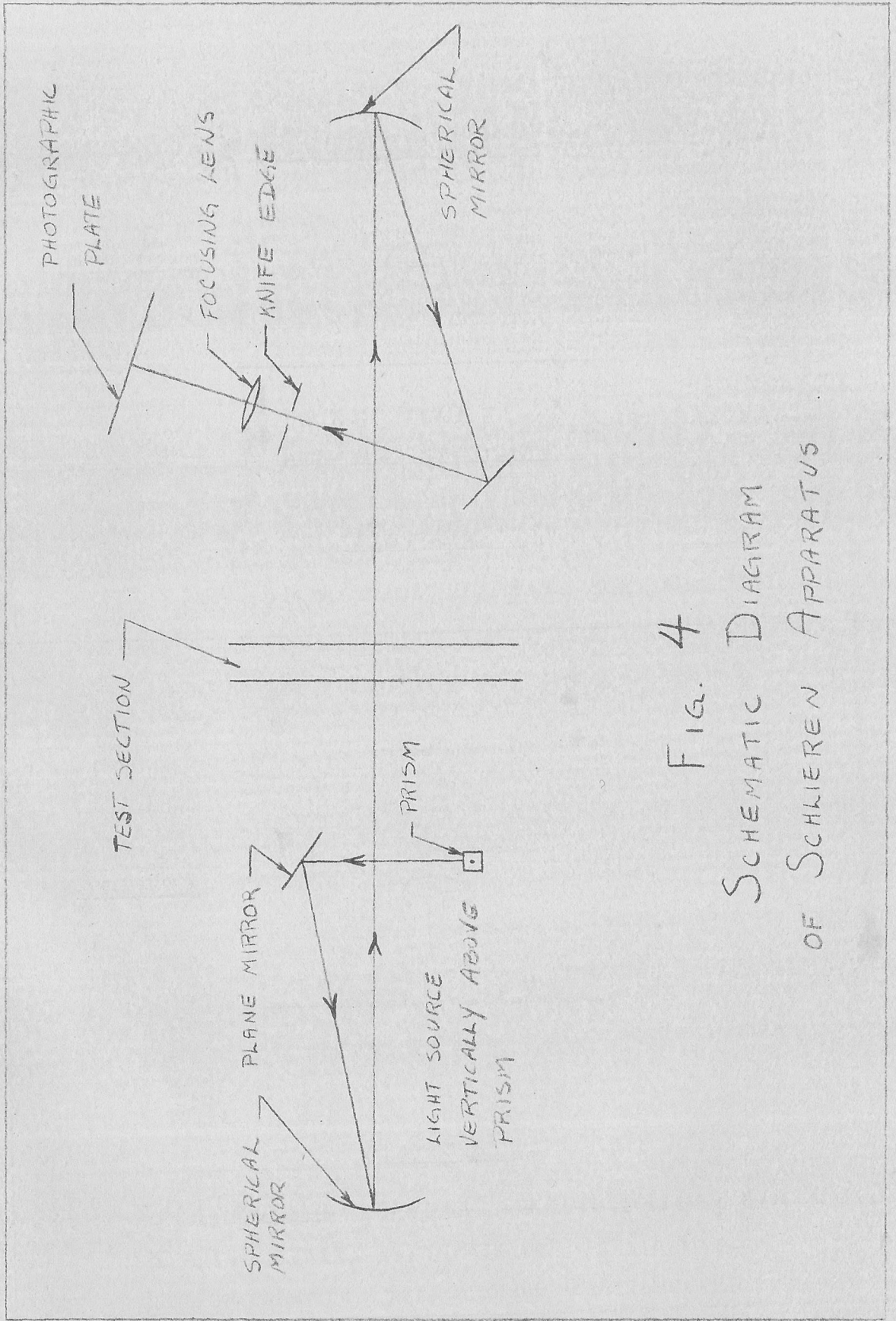


Fig. 4
 SCHEMATIC DIAGRAM
 OF SCHLIEREN APPARATUS

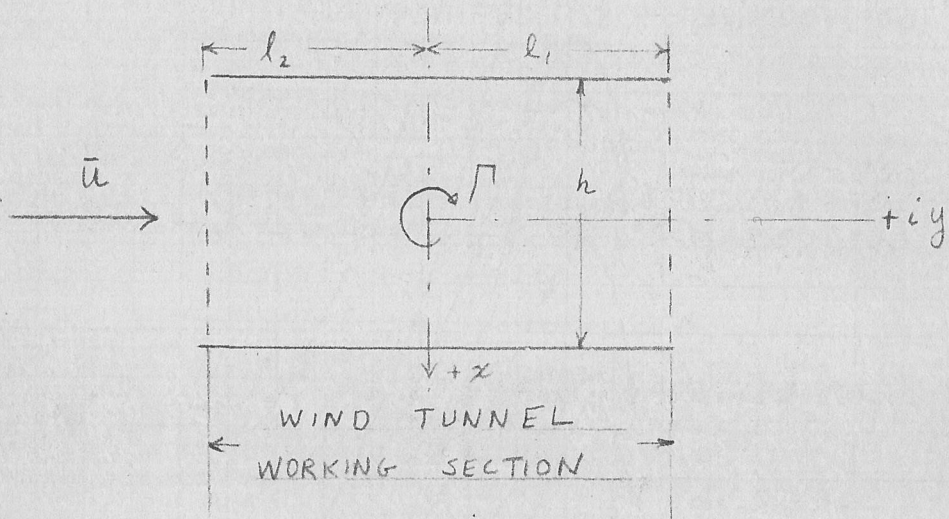


FIG. 5a

SIDE VIEW WIND TUNNEL WORKING SECTION

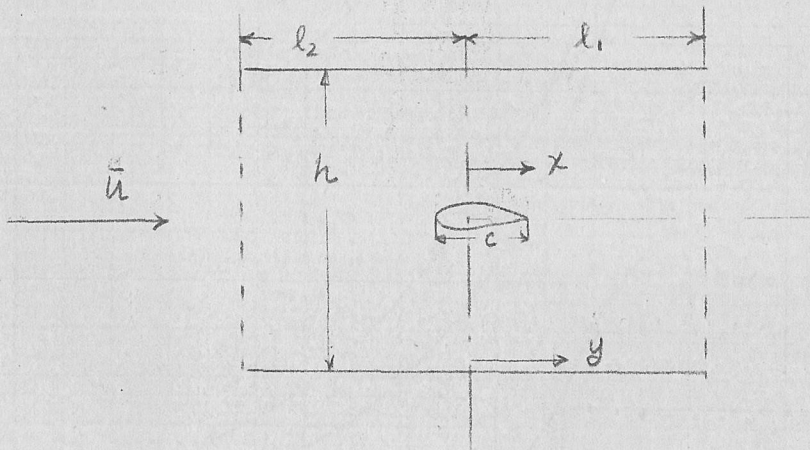
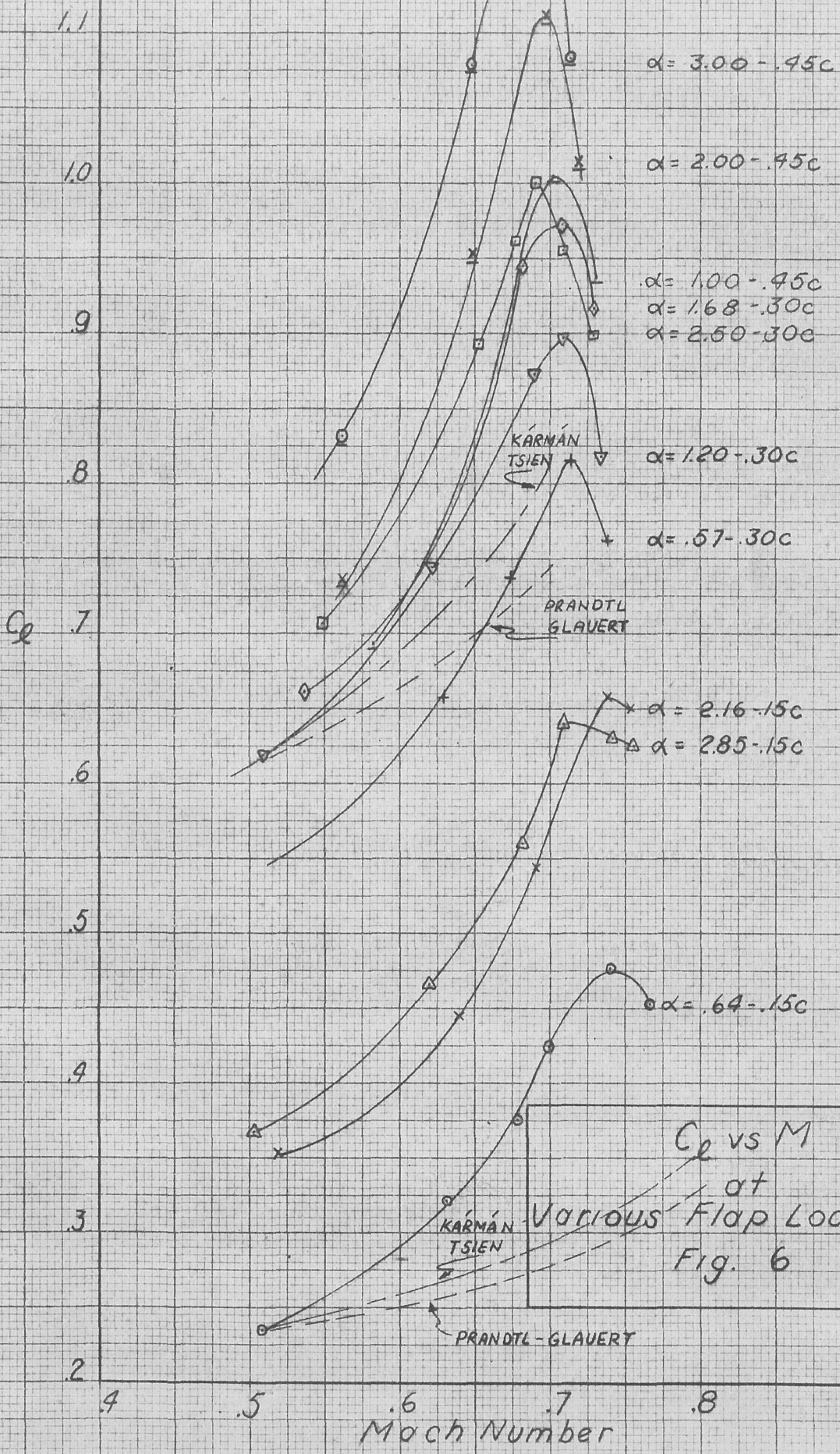


FIG. 5b

SIDE VIEW WIND TUNNEL WORKING SECTION WITH MODEL

x = coordinate for pressure distribution on airfoil

y = coordinate for pressure distribution on floor & ceiling



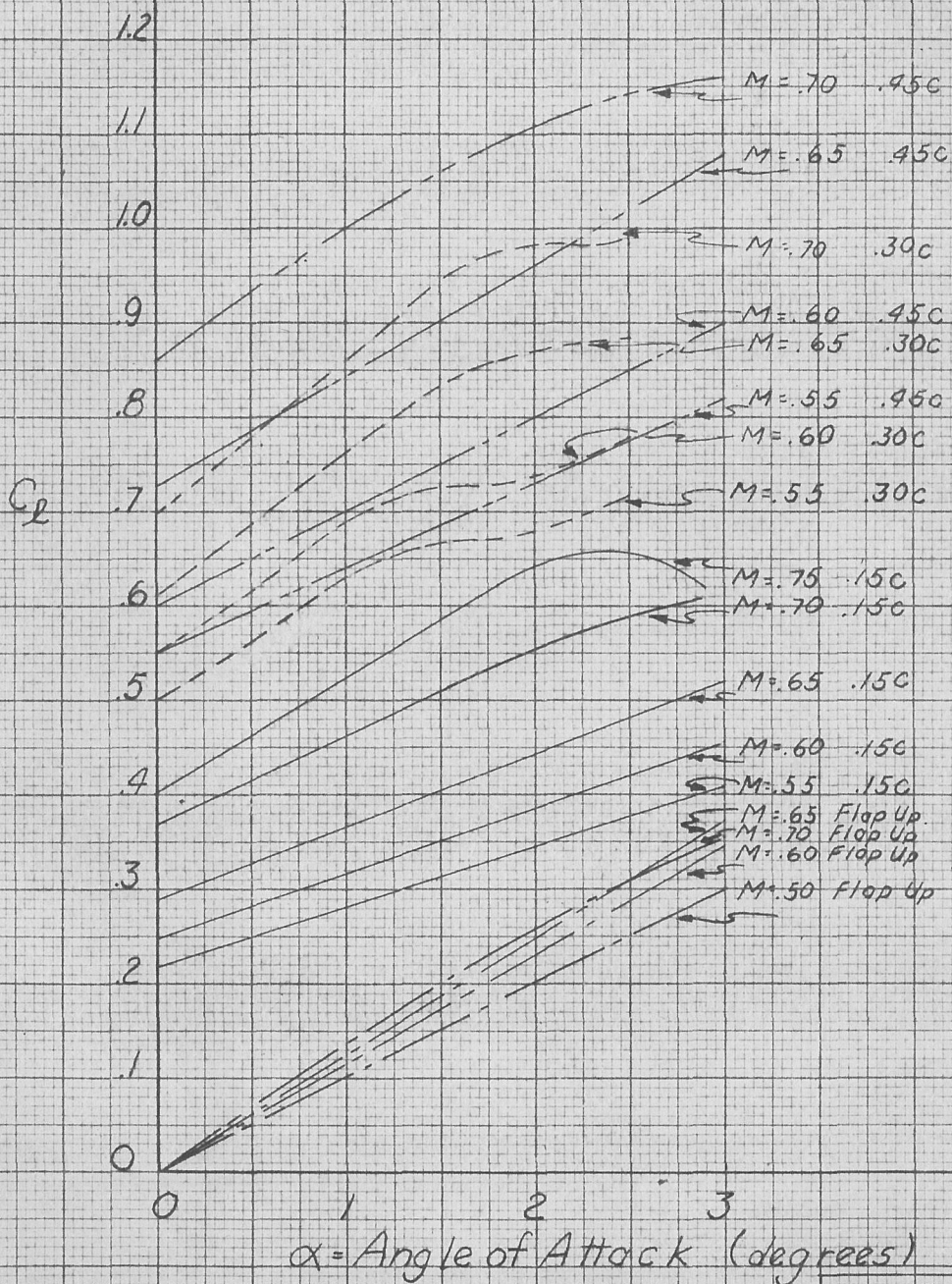


Fig. 7a
 C_L vs α

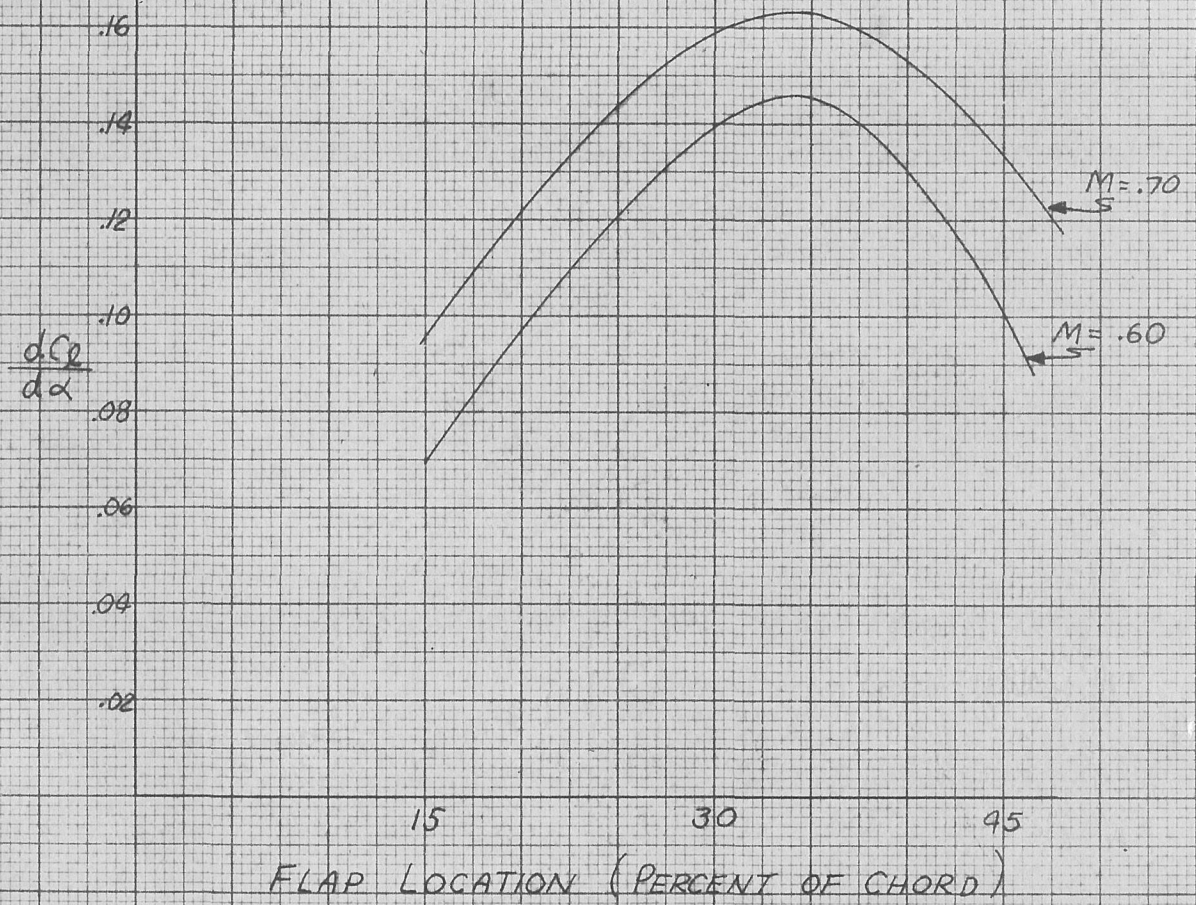
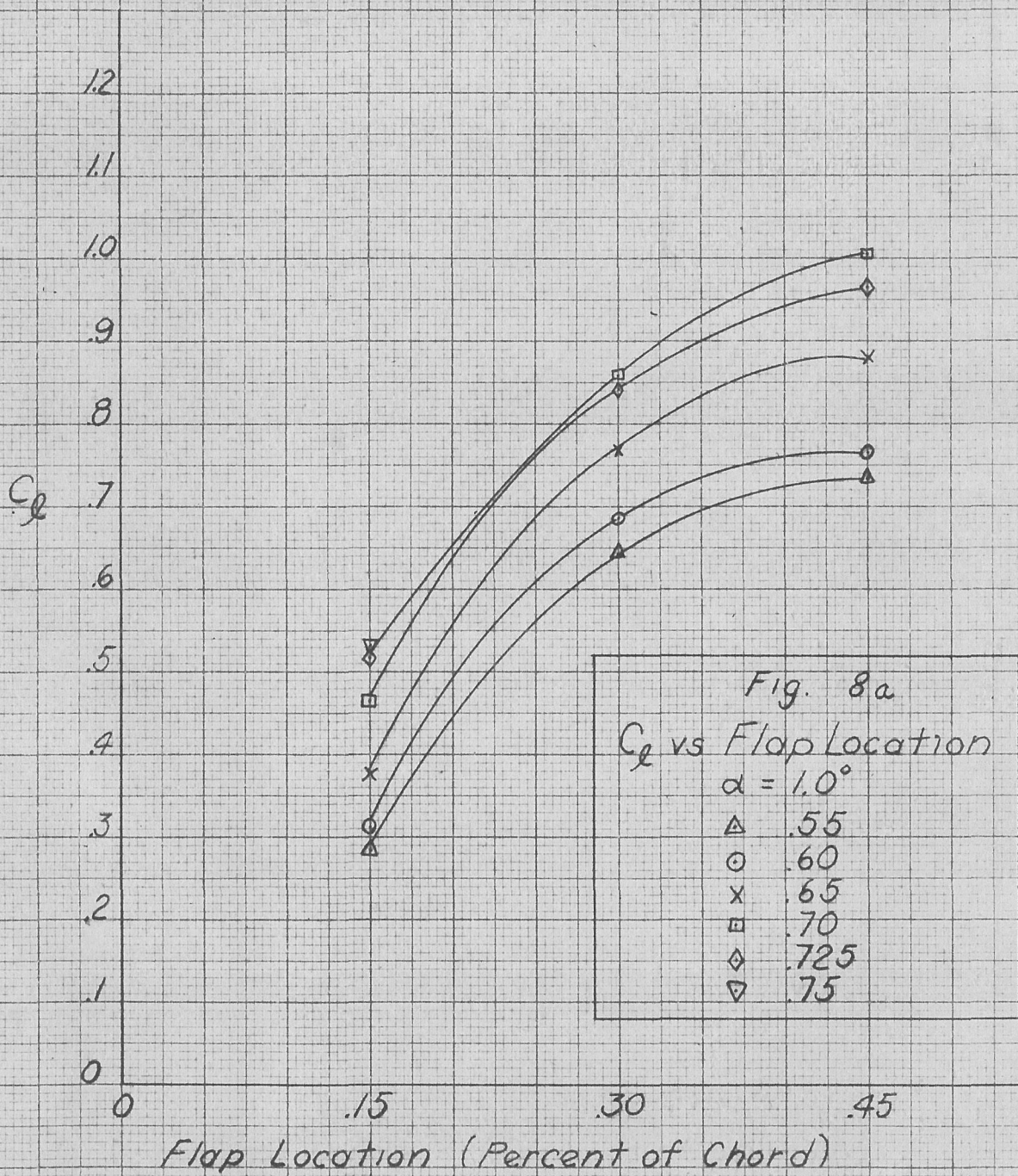


FIG 7b
 $\frac{dC_l}{d\alpha}$ VERSUS FLAP
 LOCATION



1.2
 1.1
 1.0
 .9
 .8
 .7
 .6
 .5
 .4
 .3
 .2
 .1
 0

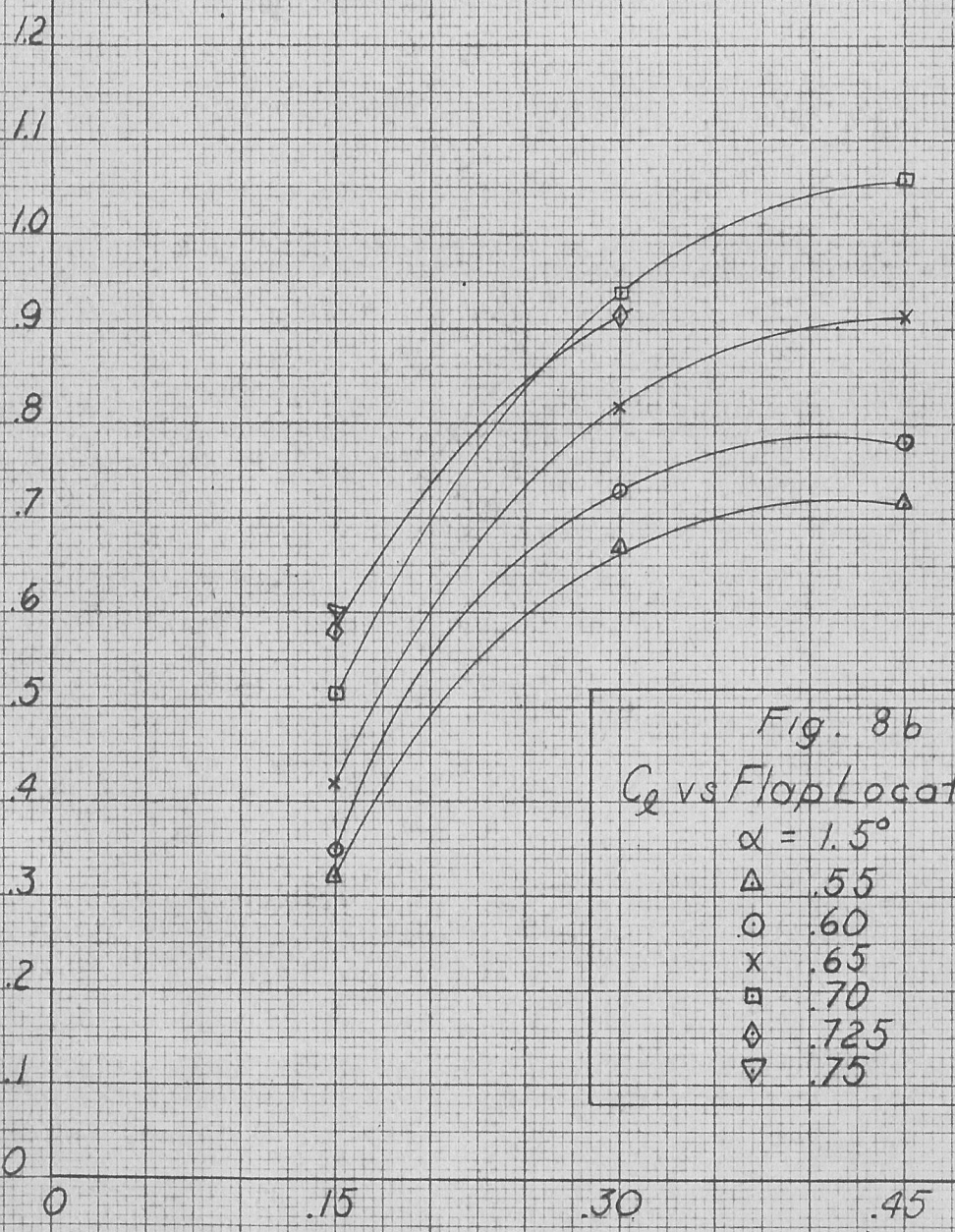
0 .15 .30 .45
 Flap Location (Percent of Chord)

C_D

1.2
1.1
1.0
.9
.8
.7
.6
.5
.4
.3
.2
.1
0

Flap Location (Percent of Chord)

Fig. 8b
 C_D vs Flap Location
 $\alpha = 1.5^\circ$
 Δ .55
 \circ .60
 \times .65
 \square .70
 \diamond .725
 ∇ .75



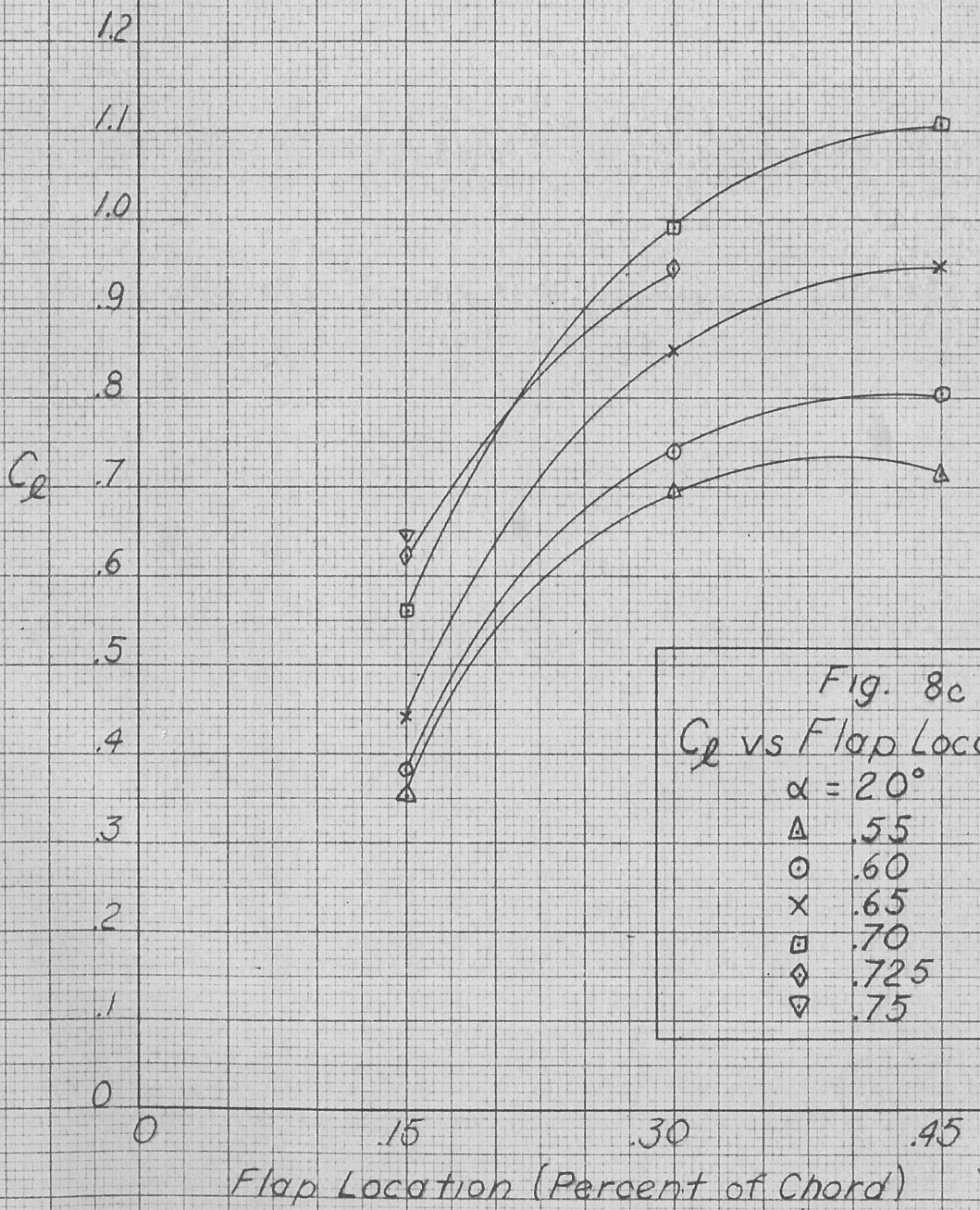


Fig. 8c
 C_L vs Flap Location
 $\alpha = 20^\circ$
 Δ .55
 \circ .60
 \times .65
 \square .70
 \diamond .725
 ∇ .75

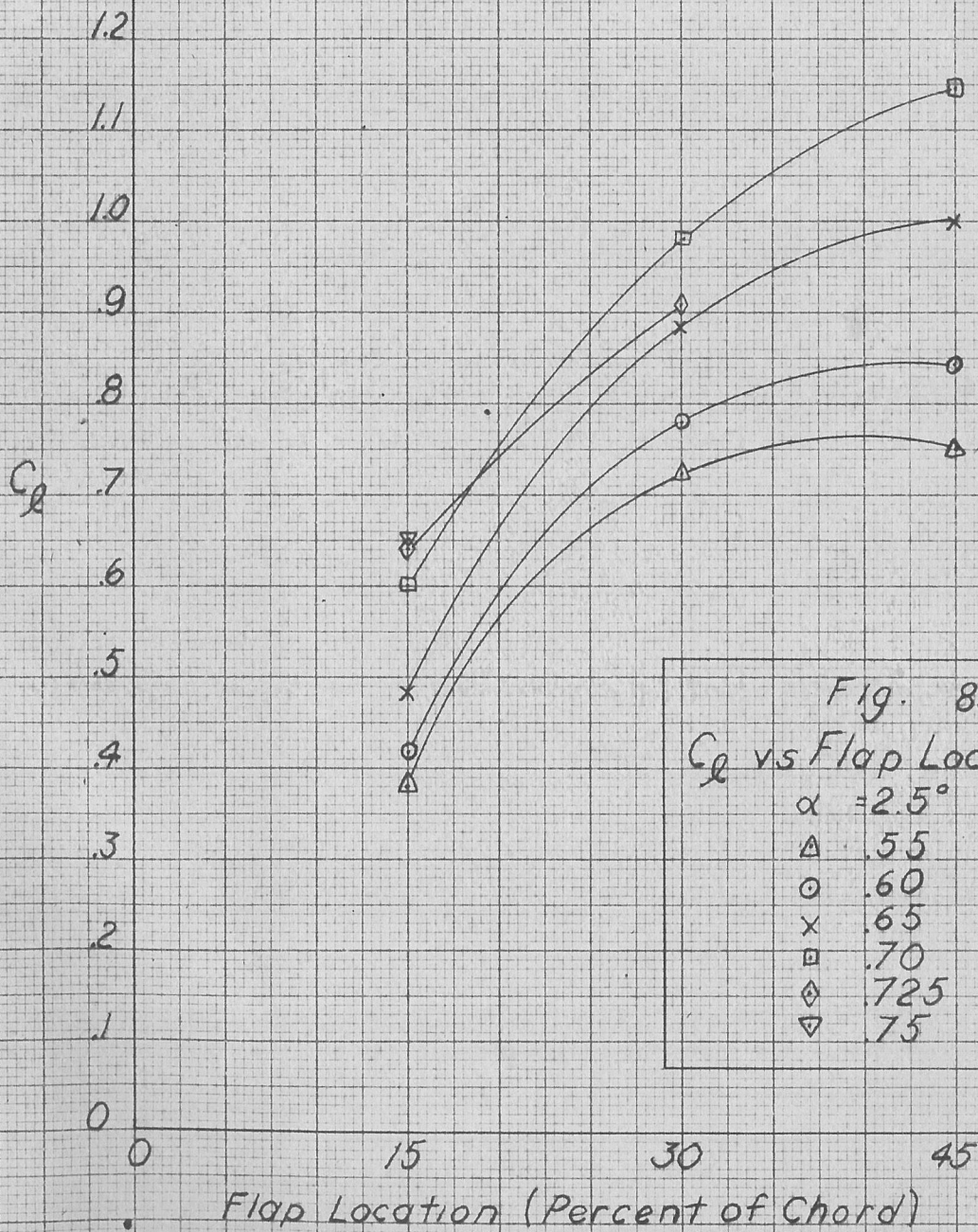


Fig. 8d
 C_L vs Flap Location
 $\alpha = 2.5^\circ$
 Δ .55
 ○ .60
 × .65
 ◻ .70
 ◇ .725
 ▽ .75

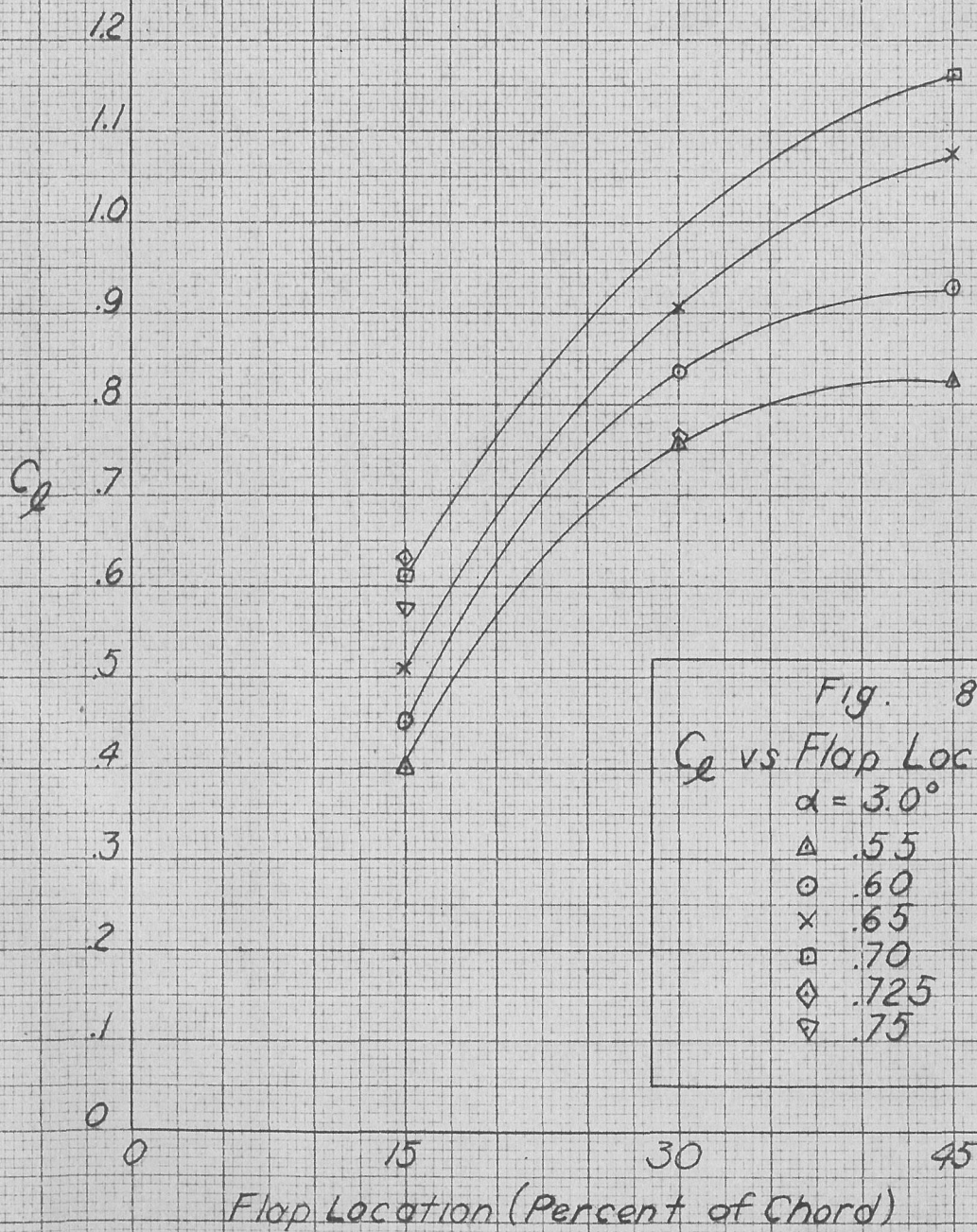


Fig. 8e
 C_l vs Flap Location
 $\alpha = 3.0^\circ$
 Δ .55
 \circ .60
 \times .65
 \square .70
 \diamond .725
 ∇ .75

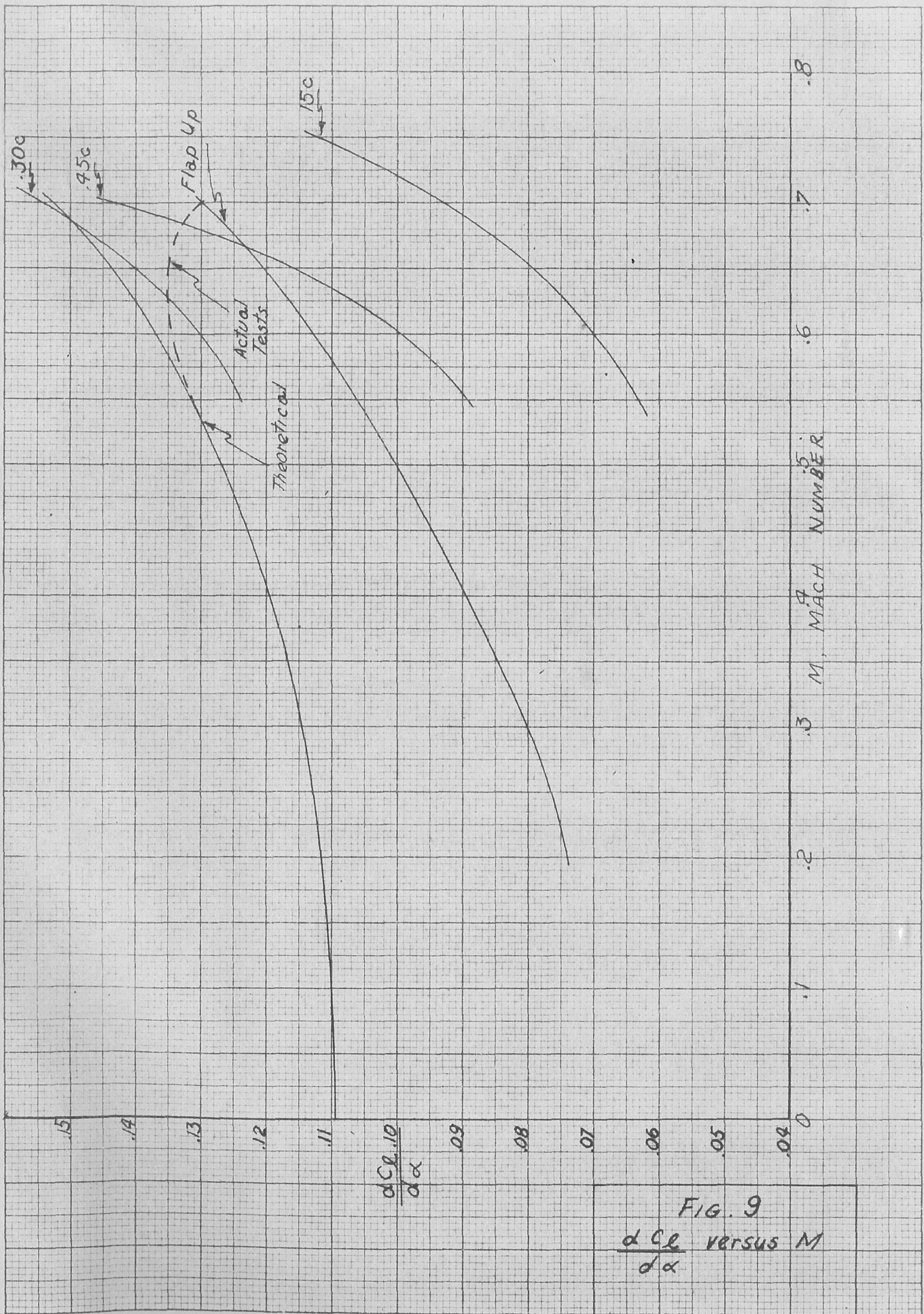


FIG. 9
 $\frac{dC_L}{d\alpha}$ versus M

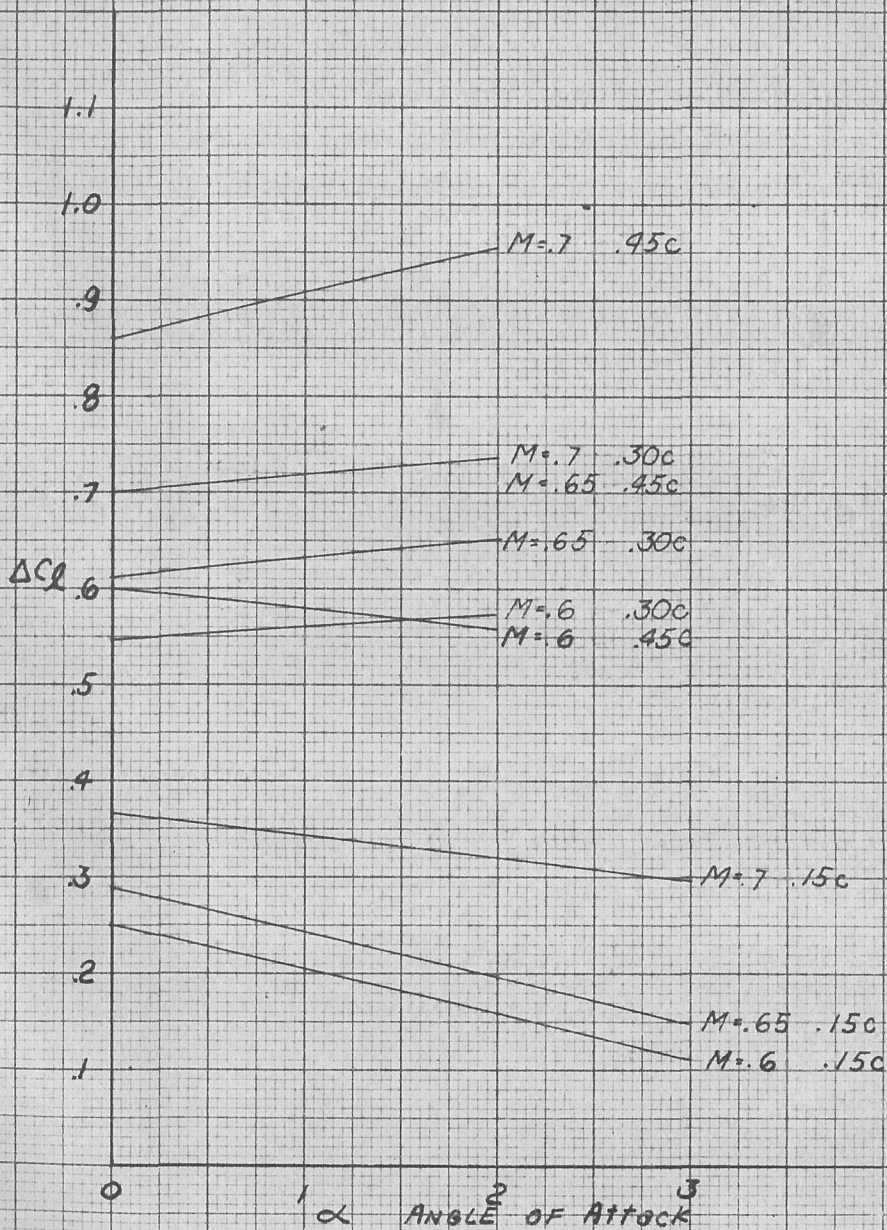
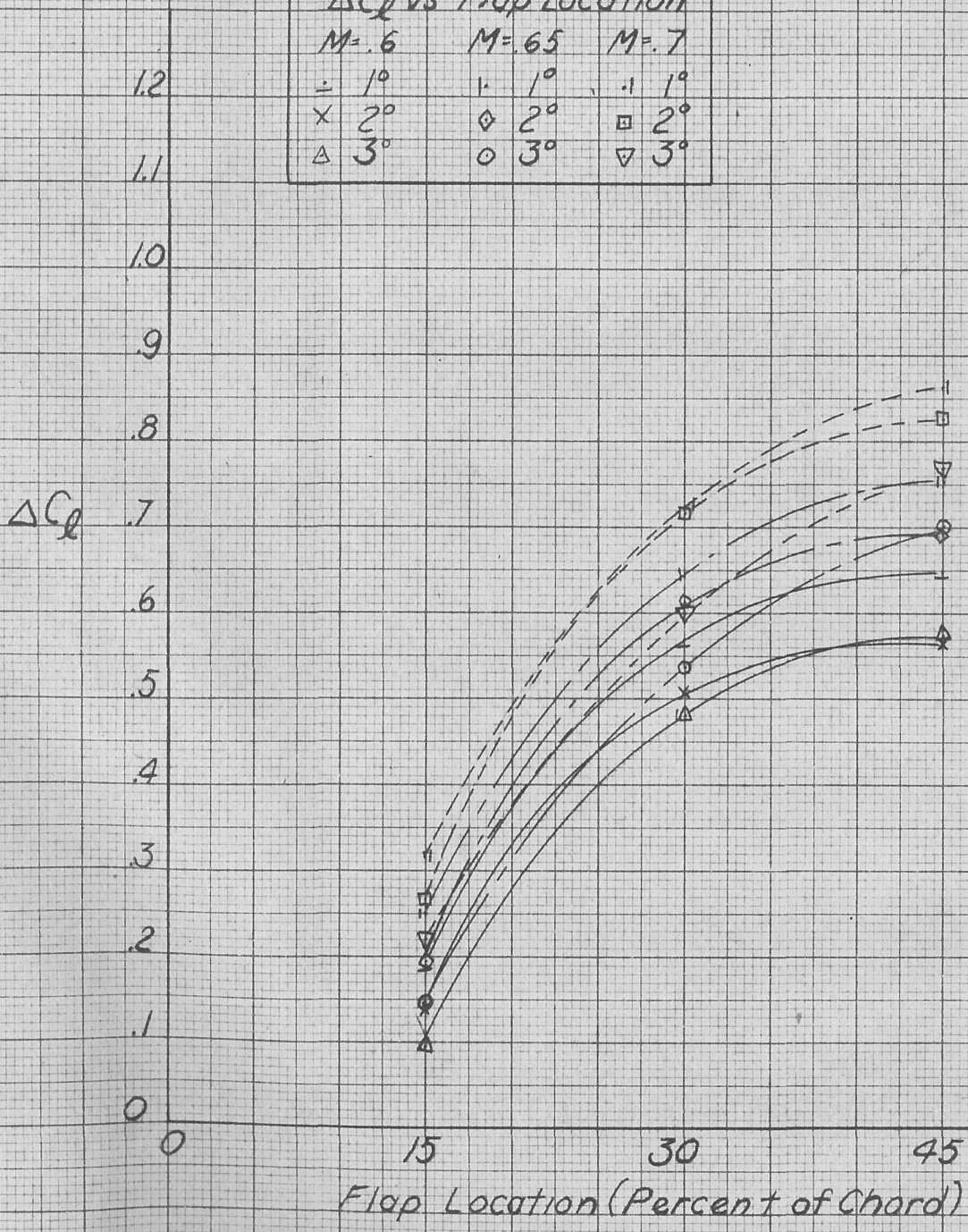
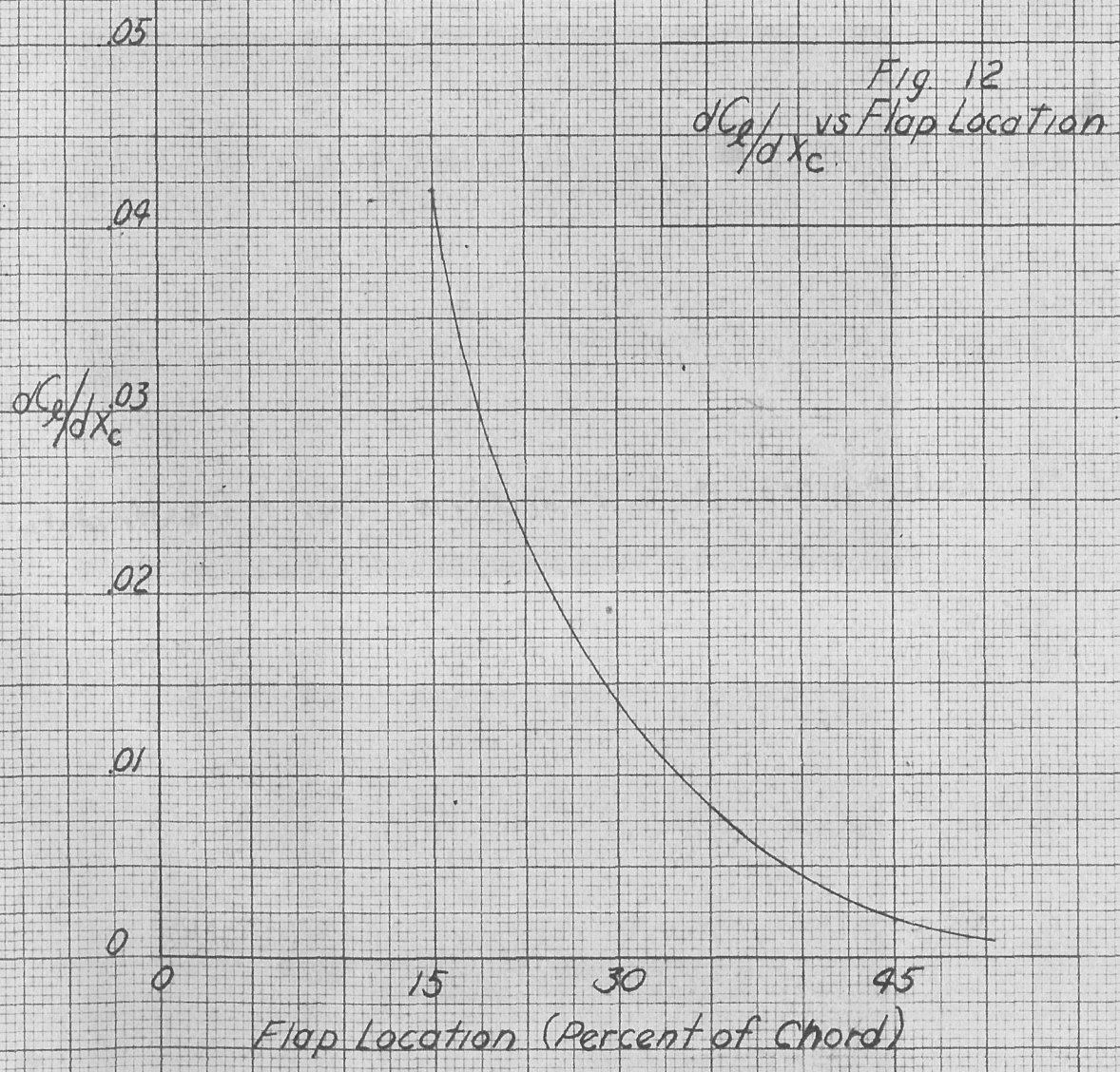


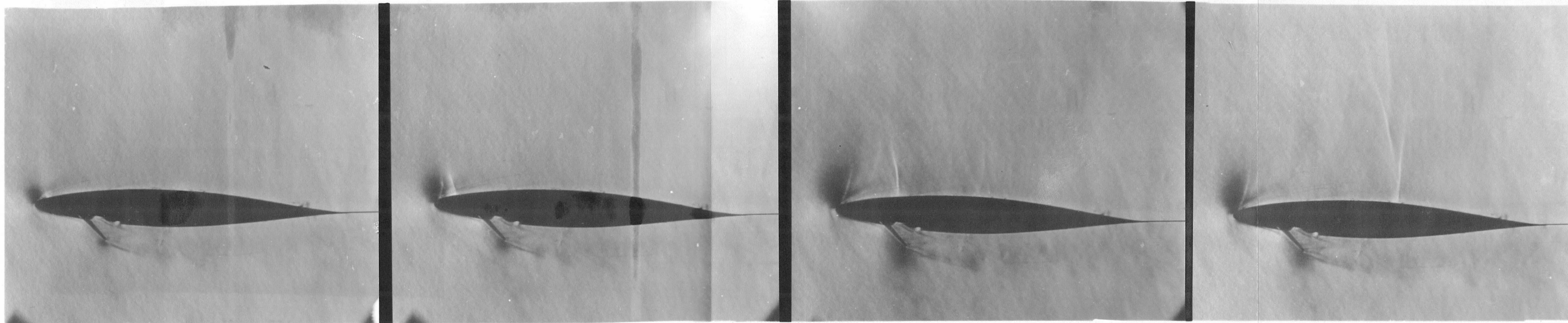
Fig 1.0
 ΔC_l vs α

Fig. 11
 ΔC_l vs Flap Location

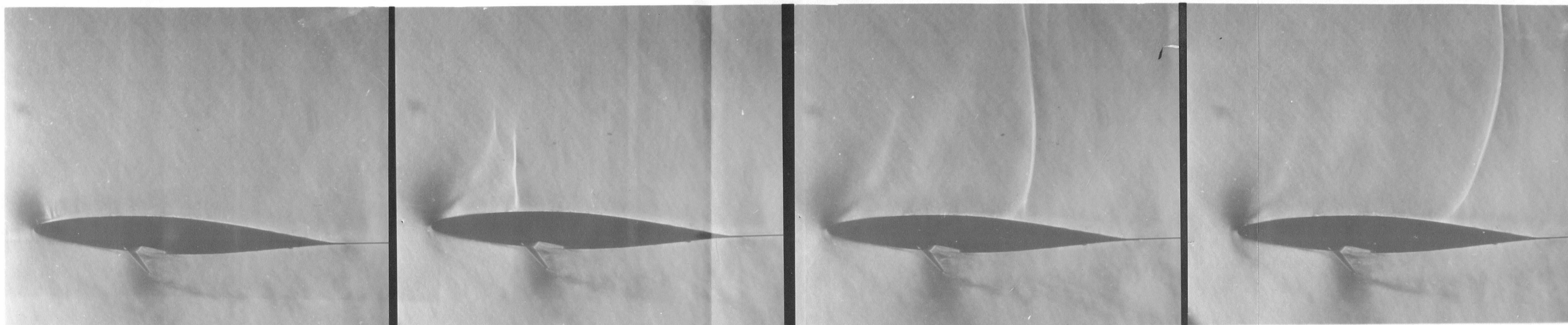
$M=0.6$	$M=0.65$	$M=0.7$
\div 1°	\cdot 1°	\cdot 1°
\times 2°	\diamond 2°	\square 2°
Δ 3°	\circ 3°	∇ 3°



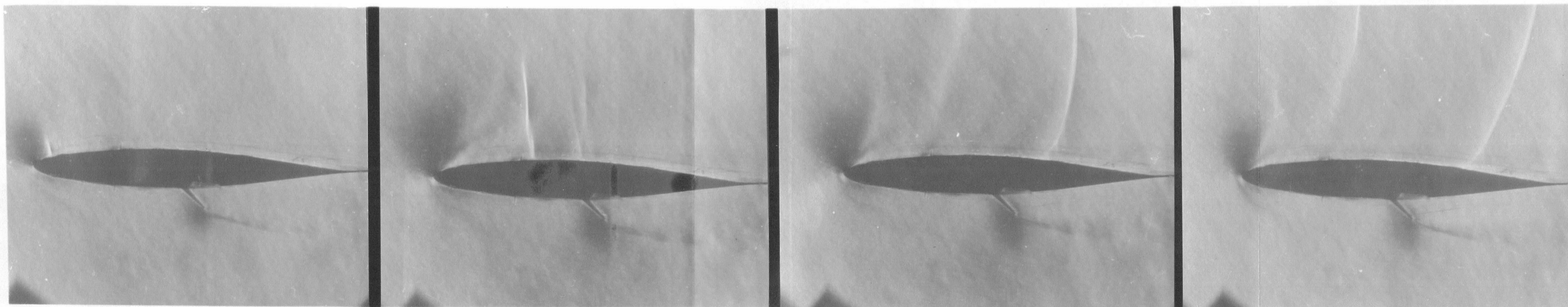




.15c



.30c



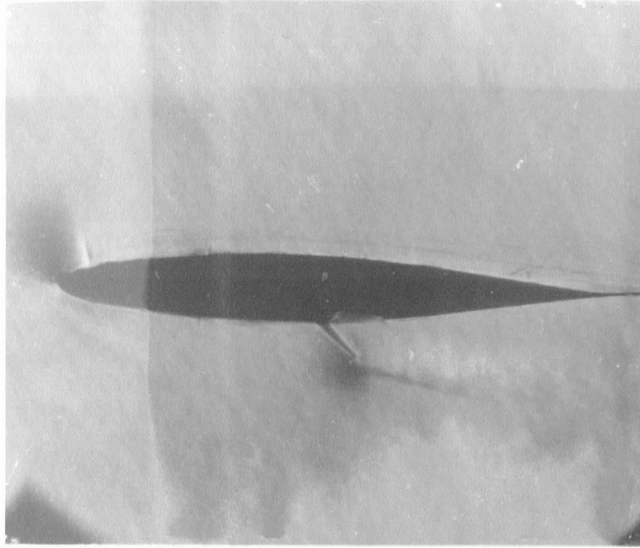
.45c

M = .561

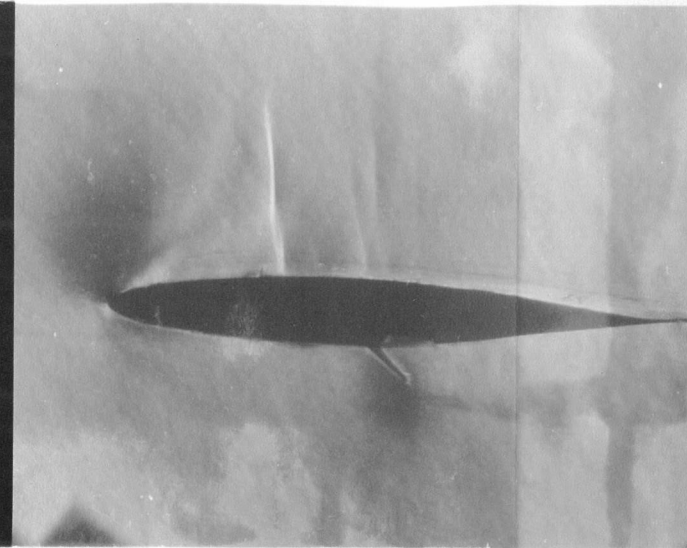
M = .648

M = .693

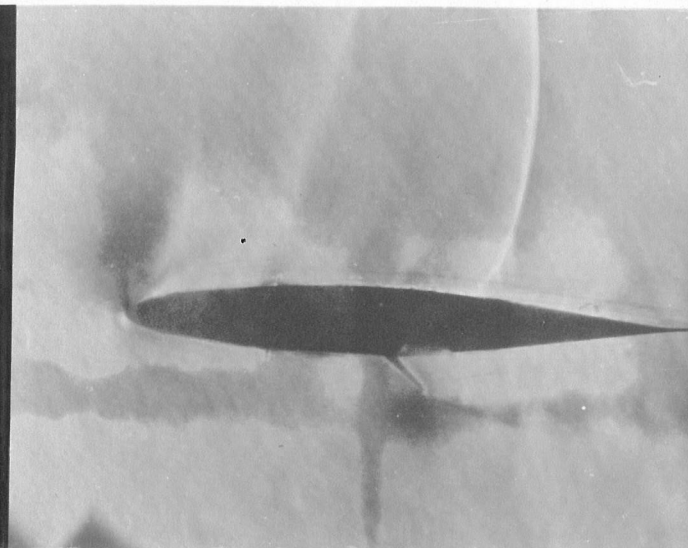
M = .714



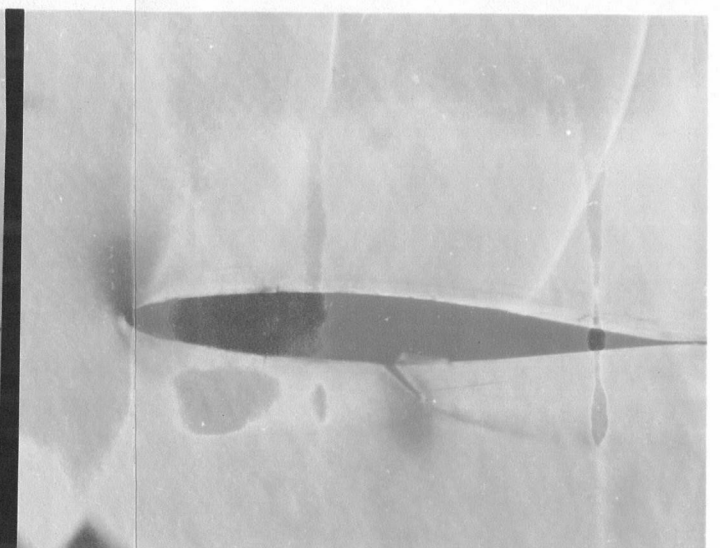
M = .562



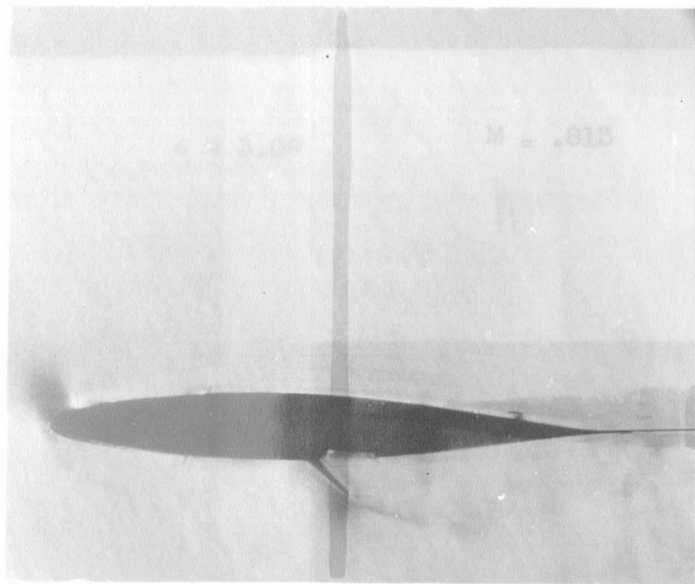
M = .648



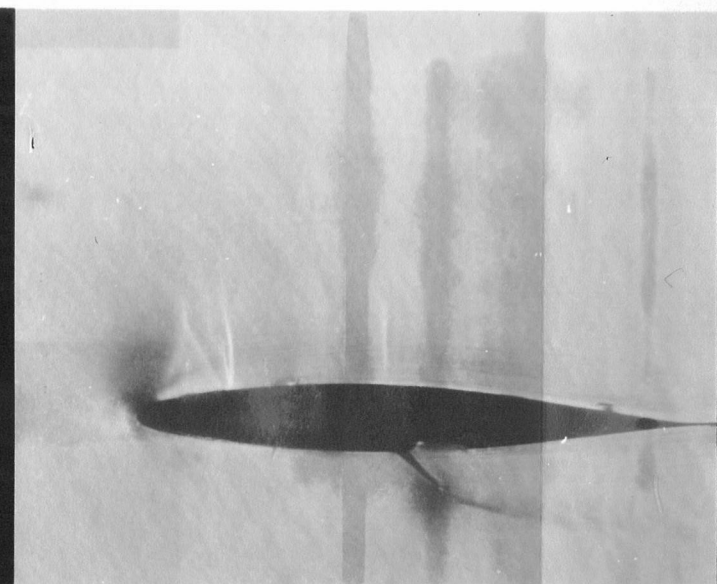
M = .692



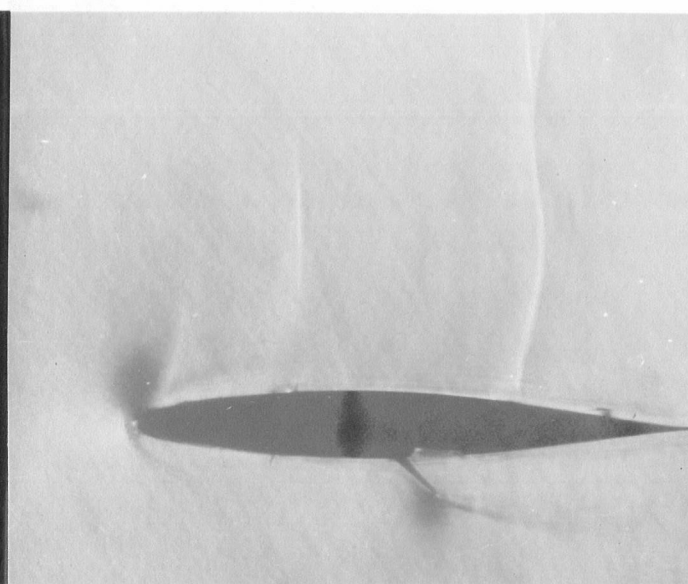
M = .714



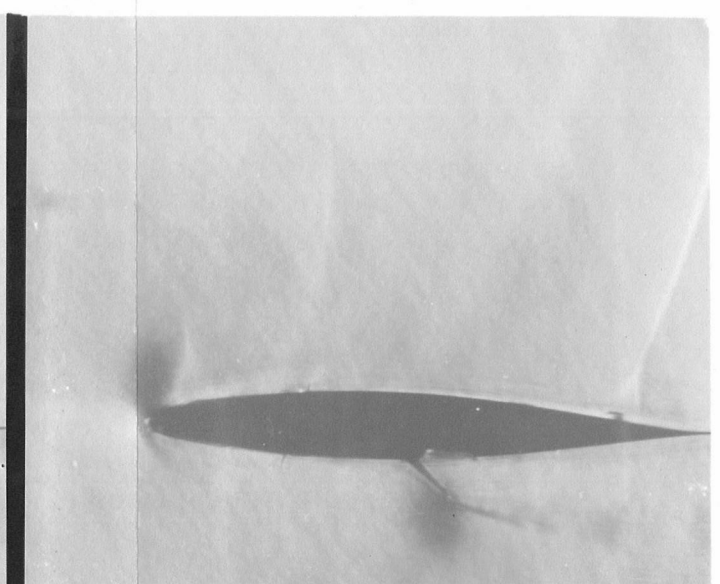
M = .564



M = .649

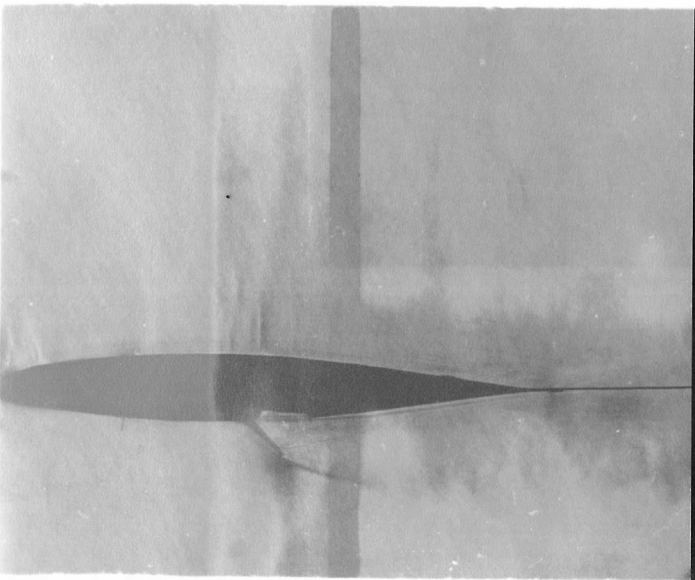


M = .696

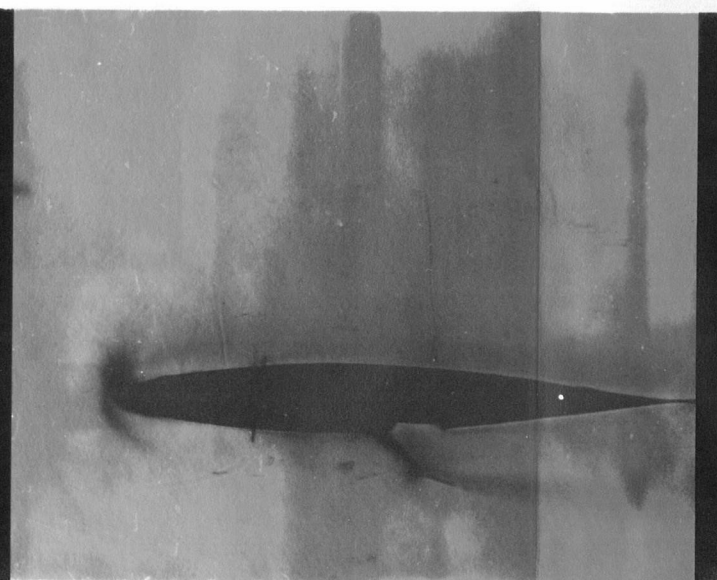


M = .719

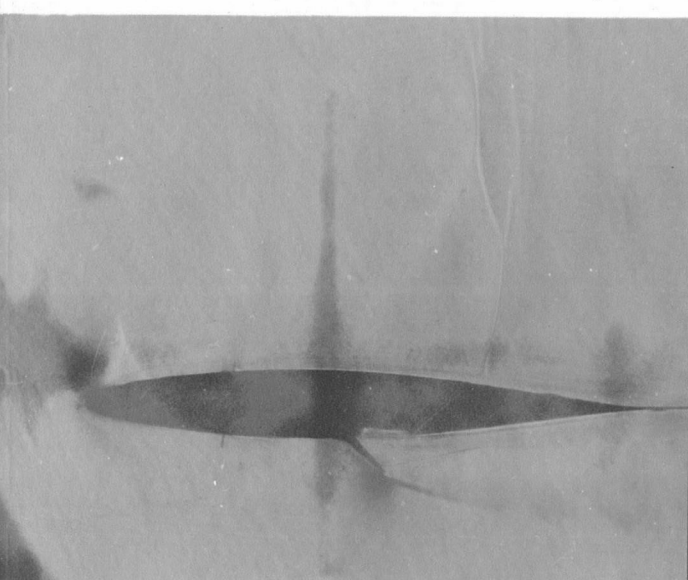
Fig. 14



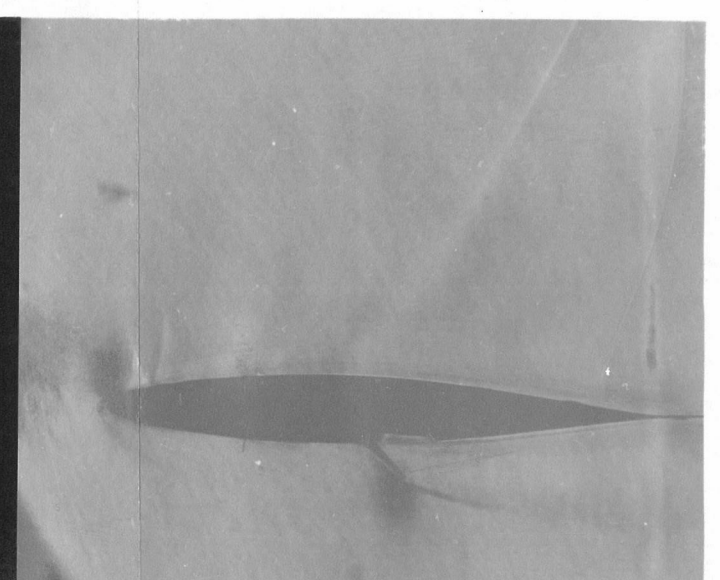
M = .657



M = .678



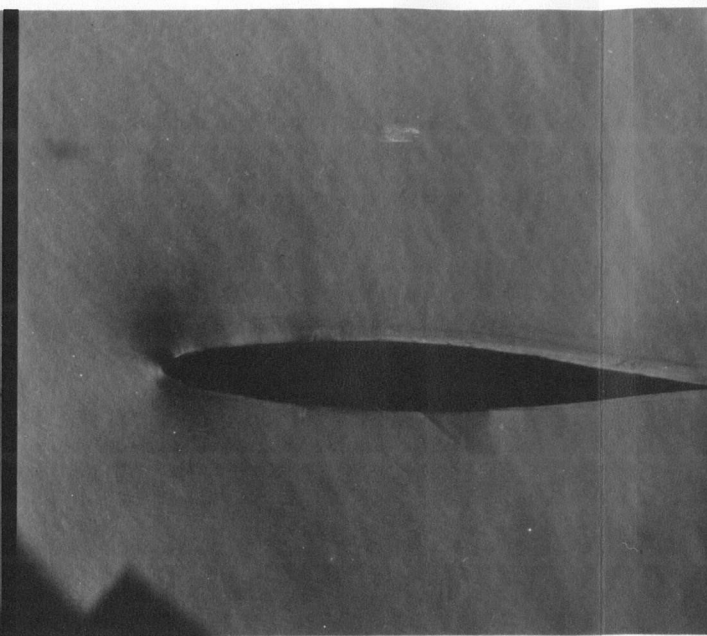
M = .701



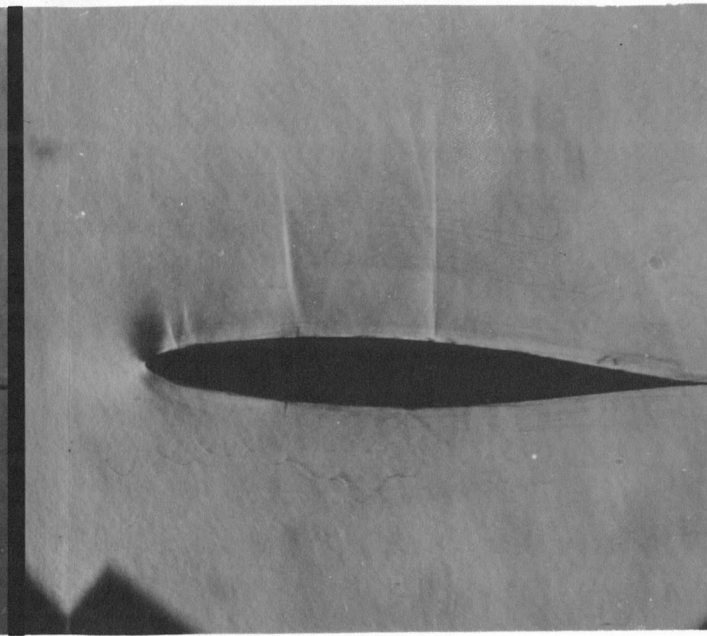
M = .730



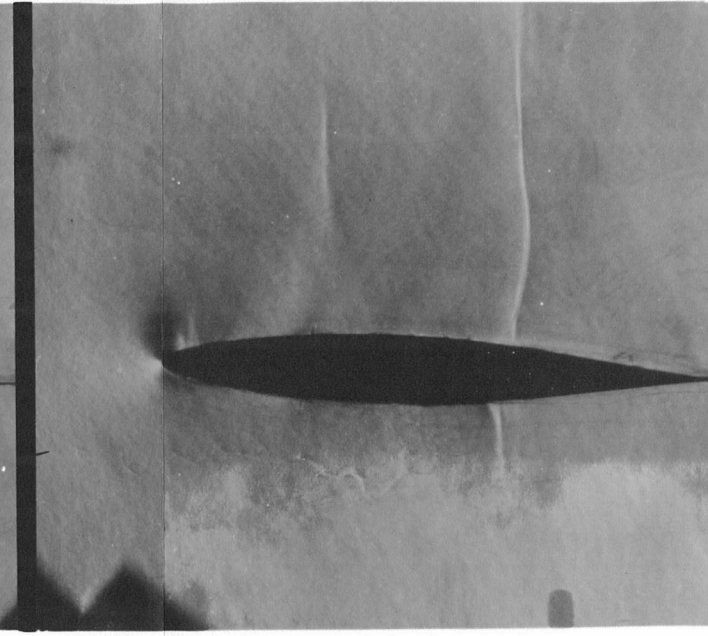
$a = 3.0^\circ$ $M = .664$



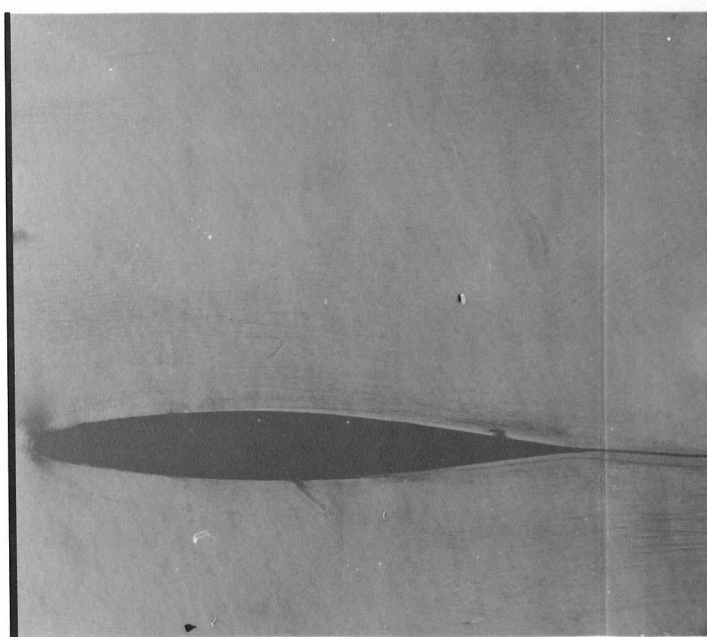
$M = .707$



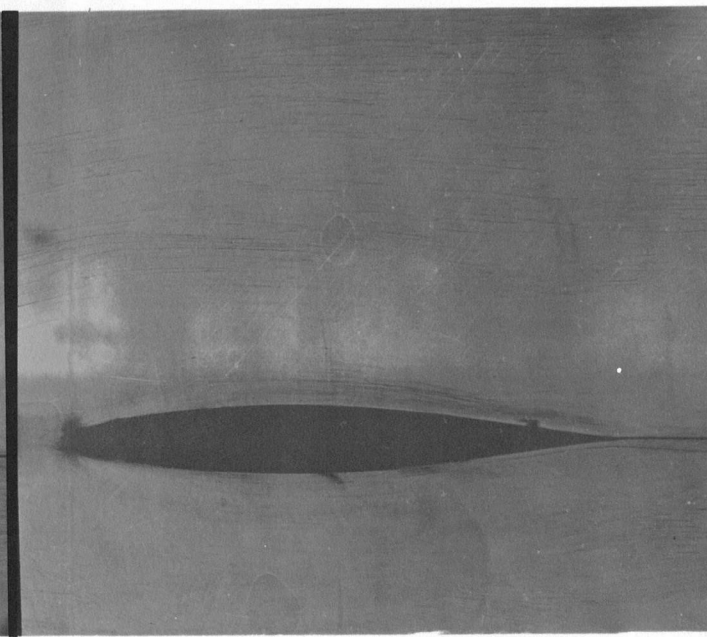
$M = .784$



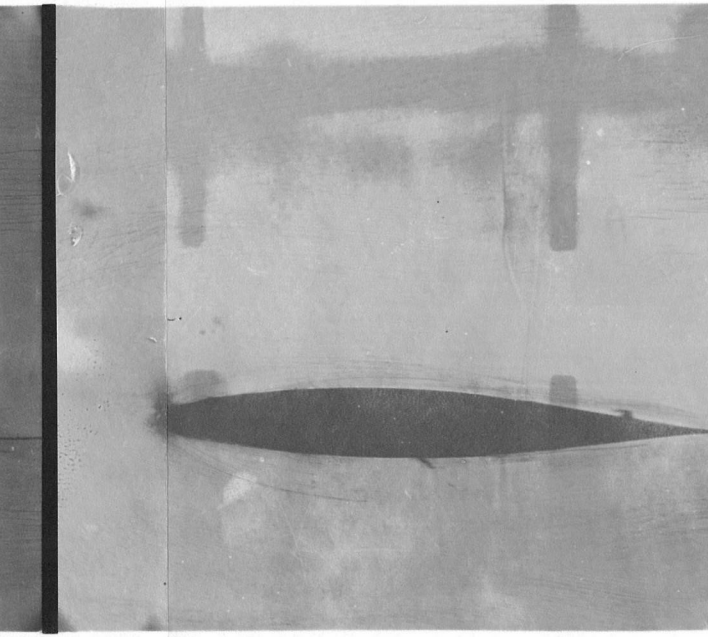
$M = .813$



$M = .708$



$M = .788$



$M = .829$ $a = 2.0^\circ$